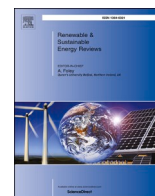


Title	Improving gaseous biofuel yield from seaweed through a cascading circular bioenergy system integrating anaerobic digestion and pyrolysis
Authors	Deng, Chen;Lin, Richen;Kang, Xihui;Wu, Benteng;O'Shea, Richard;Murphy, Jerry D.
Publication date	2020-05-11
Original Citation	Deng, C., Lin, Ri., Kang, X., Wu, B., O'Shea, R. and Murphy, Jerry D. (2020) 'Improving gaseous biofuel yield from seaweed through a cascading circular bioenergy system integrating anaerobic digestion and pyrolysis', Renewable and Sustainable Energy Reviews, 128, 109895 (20 pp). doi: 10.1016/j.rser.2020.109895
Type of publication	Article (peer-reviewed)
Link to publisher's version	http://www.sciencedirect.com/science/article/pii/S1364032120301878 - 10.1016/j.rser.2020.109895
Rights	2020 The Authors. Published by Elsevier Ltd. This is an open access article under the CC BY license. (http://creativecommons.org/licenses/by/4.0) - http://creativecommons.org/licenses/by/4.0
Download date	2025-07-04 06:18:57
Item downloaded from	https://hdl.handle.net/10468/10200



UCC

University College Cork, Ireland
Coláiste na hOllscoile Corcaigh



Improving gaseous biofuel yield from seaweed through a cascading circular bioenergy system integrating anaerobic digestion and pyrolysis

Chen Deng^{a,b}, Richen Lin^{a,b,*}, Xihui Kang^{a,b,c,d}, Benteng Wu^{a,b}, Richard O'Shea^{a,b}, Jerry D. Murphy^{a,b}

^a MaREI Centre, Environmental Research Institute, University College Cork, Cork, Ireland

^b School of Engineering, University College Cork, Cork, Ireland

^c Guangzhou Institute of Energy Conversion, Chinese Academy of Sciences, Guangzhou, China

^d University of Chinese Academy of Sciences, Beijing, China

ARTICLE INFO

Keywords:

Biomethane
Anaerobic digestion
Seaweed
Biochar
Pyrolysis
Cascading circular bioenergy system

ABSTRACT

Advanced biofuels include biomass sources free from land use such as seaweed. Seaweed biomethane may contribute significantly to a climate-neutral transport future; however, seaweed has limited biodegradability via anaerobic digestion (AD). To address this issue, the authors proposed a cascading circular bioenergy system incorporating pyrolysis (Py) for production of biochar, syngas and bio-oil, with the primary use of biochar in AD to promote biomethane production through direct interspecies electron transfer. The feasibility of the proposed AD-Py system was demonstrated by integrating a seaweed-based AD and a residue-based Py system to enhance advanced biofuels production. The AD results showed biochar achieved comparable performances to high-cost graphene in terms of enhancing biomethane production from seaweed. When digesting *Laminaria digitata* (common kelp), optimal biochar addition at 1/4 (biochar mass: volatile solid of seaweed) increased biomethane yield by 17% and peak production rate by 29% with accelerated volatile fatty acids conversion during AD. When digesting *Saccharina latissima* (sugar kelp), biomethane yield increased by 16% with optimal biochar addition. A mass and energy balance analysis indicated that processing 1.000 t of *Laminaria digitata* in AD, combustion of syngas and surplus biochar (in excess of biochar added in AD) from Py of 1.254 t forest residue and 0.078 t dried digestate could fulfil all the heat demand for the integrated AD-Py system. The process integration increased biomethane yield by 17% and bio-oil yield by 10%. Furthermore, a 26% decrease in digestate mass flow could be achieved, thereby reducing the demand for agricultural land for digestate application.

1. Introduction

1.1. Advanced gaseous biofuel from seaweed

The transport sector accounted for 29% of total EU-28 CO₂ emissions in 2017 according to the International Energy Agency's statistics [1]. The development and deployment of advanced biofuels are required for climate-neutral transport, especially long-distance transport vehicles (ships, long-haul trucks and coaches). The recast Renewable Energy Directive (REDII) specifies an increase in the share of advanced biofuels in transport energy demand from 0.5% in 2021 to 3.6% by 2030, and meanwhile proposes a scale-down of food crop-based biofuels from 7% to 3.8% by 2030 [2]. As a platform technology, anaerobic digestion (AD) is capable of converting a wide range of organic substrates to biogas

(usually consisting of 50–60% biomethane), whilst providing externalities of waste treatment, improved water quality, clean air, together with rural job creation. Biogas from AD may be upgraded to biomethane (with greater than 98% CH₄) for use in natural gas vehicles (NGVs). NGVs are suitable for long haul trucks and coaches; biogas also has applications in ferries in the form of liquified biogas.

Advanced biofuels typically do not negatively impact on agricultural output as exemplified by algal biofuels. Seaweed (macro-algae) has a high photosynthetic efficiency, high productivity, and does not compete for finite arable land for food production with a growing world population [3]. Brown seaweed (Kelp) species such as *Laminaria digitata* (*L. digitata*) and *Saccharina latissima* (*S. latissima*) have been extensively assessed as potential AD feedstocks due to their abundance and high specific methane yield (SMY) [4,5]. Yields of these kelps are optimal in temperate oceanic climates such as in the north east Atlantic. It has been

* Corresponding author. MaREI Centre, Environmental Research Institute, University College Cork, Ireland.

E-mail address: richen.lin@ucc.ie (R. Lin).

<https://doi.org/10.1016/j.rser.2020.109895>

Received 6 February 2020; Received in revised form 19 April 2020; Accepted 1 May 2020

Available online 11 May 2020

1364-0321/© 2020 The Authors. Published by Elsevier Ltd. This is an open access article under the CC BY license (<http://creativecommons.org/licenses/by/4.0/>).

List of abbreviations

AD	Anaerobic digestion
Py	Pyrolysis
DIET	Direct interspecies electron transfer
NGV	Natural gas vehicle
SMY	Specific methane yield (ml/g VS)
BMP	Biomethane potential (ml/g VS)
VS	Volatile solid
MIET	Mediated interspecies electron transfer
VFA	Volatile fatty acid (mg/L)
TS	Total solid
SEM	Scanning electron microscope
BET	Brunauer-Emmett-Teller
XRD	X-ray diffraction
BI	Biodegradability index
HHV	Higher heating value (MJ/kg)
LHV	Lower heating value (MJ/kg)

S. latissima sample harvested in February was ascribed to the high levels of alginate, reflecting a low content in readily degradable laminarin and mannitol [9]. High levels of proteins in some kelps have also been observed to cause sub-optimal performance during AD due to the imbalanced C:N ratio [10]. An optimal C:N ratio of 20–30 has been suggested for a stable AD process [11,12]. A C:N ratio of less than 15 could lead to high concentrations of ammonia, which in excess of 5 g/L is deemed inhibitory [13]. The high content of slowly degradable proteins (10–20% of TS), high content of ash (33–39% of TS), and high content of polyphenols (up to 0.13% of TS) led to the low C:N ratios (6.6–13.2), high salinity (10.4 ± 0.10 – 11.0 ± 0.08 g/L), and antimicrobial environment during the digestion of winter/spring harvested *L. digitata*, all of which were responsible for the low SMYs [14]. High content of sulphur and chloride may also raise issues for kelp digesters. In the work by Ometto et al. [15], as the addition ratio of *S. latissima* (with a sulphur content of 3.4% of TS) increased from 20% to 80% (VS percentage of *S. latissima* in the mixed feedstock) into the semi-continuous AD reactors treating municipal wastewater sludge, the hydrogen sulphide in the biogas significantly increased from nearly zero to 10 000 ppm, well above the critical threshold for inhibition (200 ppm [13]). In a previous study by Tabassum et al., the chloride concentration

Table 1
Specific biomethane yield of *L. digitata* and *S. latissima* during anaerobic digestion (AD) in different studies.

Seaweed species	Month of harvest	AD temperature	SMY (ml/g VS)	Biodegradability index (%)	Reference
<i>L. digitata</i>	August	37 °C	218.0	46	[6]
<i>L. digitata</i>	January	37 °C	129.1	\	[24]
<i>L. digitata</i>	Every month throughout a year	24 °C	196.3–254.1	54–64	[25]
<i>L. digitata</i>	May	35 °C	184	\	[26]
<i>L. digitata</i>	May	45 °C	141	\	[26]
<i>L. digitata</i>	March	37 °C	245	52	[27]
<i>L. digitata</i>	September	37 °C	280	62	[27]
<i>L. digitata</i>	Every month throughout a year	37 °C	203–327	44–72	[14]
<i>L. digitata</i>	November	55 °C	155.3	72	[28]
<i>S. latissima</i>	August	37 °C	341.7	81	[6]
<i>S. latissima</i>	\	35 °C	335	\	[29]
<i>S. latissima</i>	July	35 °C	270	\	[30]
<i>S. latissima</i>	July	35 °C	209	\	[31]
<i>S. latissima</i>	August	37 °C	223	\	[32]
<i>S. latissima</i>	August	39 °C	372	\	[33]
<i>S. latissima</i>	February, May, August, and October	37 °C	195–352	\	[9]

Note: SMY: specific methane yield.

shown that *S. latissima* may produce 10250 m³ CH₄ per hectare of sea per year (365 GJ/ha/year) in Ireland [6], a number comparable to the highest range of any tropical land based liquid biofuel system. Therefore, using kelps as alternative substrates for biomethane production through innovative AD technology may significantly contribute to the fulfilment of the renewable energy targets proposed in REDII.

1.2. Challenges to biomethane production from *L. digitata* and *S. latissima*

One issue is the variability in biomethane yield of similar species in the literature as shown in Table 1. This variance may be due to the testing regime (such as the reaction temperature and inoculum to substrate ratio) and to compositional variations in harvested seaweed due to age, temperature of water, and season. Most of these SMYs accounted for a relative low percentage of the theoretical biomethane potential [7]. Allen et al. [6] showed a biodegradability of *L. digitata* of 48%, while *S. latissima* had an 81% biodegradability. The relatively low bioconversion efficiencies may be primarily attributed to: (1) the presence of complex polysaccharides, (2) an imbalanced carbon-to-nitrogen (C:N) ratio, and (3) high levels of sulphur, polyphenols and salinity. Generally speaking, high levels of ash with low levels of mannitol and laminarin were observed in winter harvested kelps [8]. The low SMY of the

in the reactor reached 11 g/L when the mono-digestion of *L. digitata* failed [16]. Efforts made towards improving AD efficiency typically include feedstock pre-treatment to reduce structure recalcitrance [17–19], co-digestion of seaweed with carbon rich biomass to balance the C:N ratio [20,21], and optimisation of operational parameters [22, 23]. These efforts generally require additional energy or material input, that may limit the net energy output.

1.3. Interspecies electron transfer in anaerobic digestion

Mediated interspecies electron transfer (MIET) in which two syntrophic partners (fermentative bacteria and methanogens) utilize H₂ or formate as the electron carriers is an essential process within the AD system. However, the efficiency of MIET is relatively low due to the diffusion limitation of electron carriers. Alternatively, direct interspecies electron transfer (DIET) induced by conductive carbon-based materials (such as graphene and biochar) may lead to a higher AD efficiency as DIET does not involve the production and diffusion of electron carriers. Previous studies have demonstrated that the conductive nanomaterial graphene could stimulate DIET in complex microbial communities, thereby improving AD performance [34–37]. Table 2 provides a summarised review of graphene application in AD. With graphene added at an optimal concentration, the AD performance could

Table 2

Application of graphene in batch anaerobic digestion (AD) of different substrates.

AD feedstock	AD temperature	Optimal addition ratio of graphene to feedstock	Effects on AD performance	Reference
Ethanol	35 °C	15% VS	Methane yield increased by 25%. Maximum methane production rate increased by 20%.	[36]
Glycine	35 °C	40% VS	Methane yield increased by 6%. Maximum methane production rate increased by 28%.	[34]
Acetate sodium; Glucose	35 °C	6% COD	Methane production rate increased by 25% from acetate sodium and by 51% from glucose.	[35]
Ethanol	35 °C; 55 °C	27% VS	Methane yield increased by 14% in mesophilic AD and 5% in thermophilic AD. Methane production rates enhanced by 25% in mesophilic AD and 26% in thermophilic AD.	[37]

be significantly enhanced with biomethane yield increasing by 5–25% and biomethane production rate increasing by 20–51%. It is noteworthy that the enhancement of AD performance depends highly on graphene concentration, feedstock characteristics, and AD operational conditions (such as mesophilic and thermophilic temperatures).

Despite the considerable enhancement in biomethane production, the high cost of graphene can be an obstacle to its practical application. The purchase price for graphene nanosheets was €644/kg from Sigma Aldrich [38]. The average retail price for biochar was about €3/kg according to a market survey conducted by the International Biochar Initiative in 2014 [39,40]. As a cheaper conductive and porous carbon material, biochar can be produced from pyrolysis of various lignocellulosic biomass and has the potential to exhibit a strong electron transfer capability [41,42]. In addition to stimulating DIET, biochar may mitigate feedstock-induced instability through adsorbing microbial inhibitors, enhancing the buffering capacity in the reactor, and immobilising bacterial cells due to its large specific surface area, porosity, and inherent surface chemistry [43]. These findings highlight use of biochar as a low-cost alternative additive for both inhibitor removal and establishment of DIET. Cooney et al. found that the microbial biofilms created by biochar could support the colonisation of acidogens, acetogens and methanogens at the start-up stage of the AD process, contributing to a 69% COD reduction of the high strength wastewater [44]. Wang et al. found that vermicompost derived biochar could alleviate the accumulation of volatile fatty acids (VFAs) and increase pH, thereby improving the stability of the digester at high organic loading rates [45]. From the perspective of the surface characteristics, biochar may have the potential to enhance biomethane production and stability of the AD process as compared to graphene. A gap in the state of the art is the lack of scientific literature on the effects of biochar on digestion of brown seaweed (*L. digitata* and *S. latissima*). Optimisation of biochar addition in digestion of seaweed is required to improve the biodegradability of seaweed, which in turn is required to facilitate a climate friendly and financially viable seaweed biofuel industry.

1.4. Cascading circular bioenergy system

Although AD technology is relatively mature, it is still faced with several challenges, such as process instability, inefficiency associated with the inability to digest recalcitrant feedstocks (as is the case with seaweed) and associated agricultural land banks for reuse of digestate. Digestate is dominated by undegraded or slow to degrade components of feedstocks (such as lignin, nutrients and microbial cells). If biodegradability is limited to 60% then 40% of potential energy is unutilised. Traditional land application of digestate may lead to waste in the inherent energy value of the digestate, high demand for arable land, high transportation cost of dilute digestate, and greenhouse gas emissions associated with slow to degrade undigested volatile material. The foregoing affects the sustainability of the entire supply chain [46]. Pyrolysis can extract this residual energy in the solid digestate through tuneable production of syngas, bio-oil and biochar. Bio-oil has similar molecules (such as C8 – C16 aromatics along with paraffins and cycloalkanes) to petroleum crude oil, and has potential for use in hard to decarbonise transport sectors such as shipping and aviation [47]. Biochar is a sustainable carbonaceous material with applications in diverse areas, including for, supercapacitors, solid carbon catalysts, improving soil organic content and biological technologies. Application of biochar to soil not only improves soil quality but is deemed a negative emission technology through carbon sequestration [48,49]. Biological technologies such as addition of biochar to an AD process could enhance biomethane production and support the development of stable microbial communities. Biochar can link biological AD and thermochemical pyrolysis in a cascading circular AD-Py system, which may have many benefits including: overcoming recalcitrant features of feedstock; reduction of problematic land application for digestate management; improvement in biofuel production and energy recovery efficiency; and increased economic benefits within the circular bioenergy system. Previous studies have shown that integrating AD and Py could increase energy recovery under optimised conditions [50]. However, the efficiency of an integrated AD-Py system depends on many factors, such as the biodegradability of the feedstock, the allocation of biomass resources to the AD and Py processes, and the interactions between the two processes under different integration scenarios. The efficiency of an integrated AD-Py process based on innovative third-generation feedstock seaweed has not been documented in the literature yet.

1.5. Research gap in the state of the art and novelty of this study

The incorporation of biochar into the digester and the reuse of digestate in the pyrolyzer offers a promising opportunity to enhance advanced biofuel production from seaweed in a cascading circular AD-Py system. However, a gap in the state of the art is an assessment of the feasibility of integrating a seaweed-based AD process and a residue-based pyrolysis process.

The innovation of this study is the optimisation of the anaerobic digestion of seaweed through biochar induced DIET and the proposition of a model for an integrated AD-Py process for co-production of advanced biofuels in the form of biomethane and bio-oil. The detailed objectives are to:

- (1) Evaluate the feasibility of using biochar as a replacement for graphene to enhance biomethane production via DIET in AD;
- (2) Assess the effects of biochar addition on biomethane production from two brown seaweed species *L. digitata* and *S. latissima*;
- (3) Demonstrate the mass and energy balance of the cascading circular AD-Py system in terms of advanced biofuels production, process efficiency, and digestate valorisation.

2. Materials and methods

2.1. Materials

The seaweed samples of *L. digitata* and *S. latissima* were naturally beach harvested in west Cork, Ireland. *L. digitata* was collected in May and *S. latissima* was collected in June. Seaweed samples were washed with tap water to remove surface impurities and subsequently cut into small particles of less than 4 mm in diameter as described by Tabassum et al. [51]. The samples were stored at $-20\text{ }^{\circ}\text{C}$ before use. The inoculum used in the biomethane potential (BMP) assays was originally sourced from an Irish farm digester and was acclimatized in a lab-scale continuous stirred tank reactor processing cellulose at $37\text{ }^{\circ}\text{C}$. The inoculum was degassed for 7 days prior to the BMP assays.

The biochar was sourced from a local pyrolysis plant (Premier Green Energy) processing waste wood. Pyrolysis was conducted in a rotary kiln system operated at $700\text{ }^{\circ}\text{C}$. Approximately 7 kg biochar was produced per hour from 30 kg of waste wood. Syngas was concomitantly produced with a heating value of 15 MJ/m^3 . The produced biochar and syngas were then combusted in the plant to provide heat for the pyrolysis reactor. The derived biochar sample was ground and sieved to ensure a particle size of $75\text{--}500\text{ }\mu\text{m}$. Graphene nanoplatelets with a particle size of $2\text{ }\mu\text{m}$ were purchased from Sigma Aldrich. Both the biochar and graphene samples were oven dried at $105\text{ }^{\circ}\text{C}$ for 12 h before use.

2.2. Biomethane potential assays

Four automatic methane potential test systems (Bioprocess AMPTS II) were used to conduct the BMP assays using seaweed as feedstock. One set can accommodate 15 glass bottle reactors, each of which has a working volume of 400 ml and a head space of 250 ml. In total 60 glass bottle reactors were available in the experimental process; a total of 19 assays in triplicate utilised 57 such reactors.

To compare the effects of graphene and biochar on AD of *L. digitata*, 26.3 g of wet *L. digitata* feedstock (containing 2.0 g of VS) and 308.0 g of inoculum (containing 4.0 g of VS) were added into each reactor (inoculum to feedstock ratio of 2:1). Then different dosages of graphene or biochar were added into each reactor: Group 1 to 5 contained 0.125, 0.250, 0.500, 2.000, and 4.000 g of graphene, respectively; Group 6 to 10 contained 0.125, 0.250, 0.500, 2.000, and 4.000 g of biochar, respectively. The addition ratio of graphene (or biochar) was defined as the mass ratio of graphene (or biochar) to the VS of seaweed. Therefore, the addition ratios of graphene in Group 1 to 5 were 1/16, 1/8, 1/4, 1/1, and 2/1, respectively. The addition ratios of biochar in Group 6 to 10 were also 1/16, 1/8, 1/4, 1/1, 2/1, respectively. A control group of *L. digitata* (Group 11, no graphene or biochar addition) was operated with 26.3 g of wet *L. digitata* and 308.0 g of inoculum.

To evaluate the effects of biochar on the digestion of *S. latissima*, 19.8 g of wet *S. latissima* feedstock (containing 2.0 g of VS) and 308.0 g of inoculum (containing 4.0 g of VS) were added into each reactor; then different dosages of biochar were added: Group 12 to 16 contained 0.125, 0.250, 0.500, 2.000, and 4.000 g biochar (equivalent to addition ratios of 1/16, 1/8, 1/4, 1/1, and 2/1), respectively. A control group of *S. latissima* digestion (Group 17, no graphene or biochar addition) was operated with 19.8 g of *S. latissima* and 308.0 g of inoculum. A positive reference group (Group 18) was operated with 2.0 g of cellulose and 308.0 g of inoculum. A blank group (Group 19) was operated with only 308.0 g of inoculum. A summary of the BMP experimental design can be found in Table S1 in the supplementary material.

Deionized water was used to adjust the working volume in each reactor. After the measurement of initial pH (approximately 8.70), the reactors were sealed and purged with N_2 to create an anaerobic environment. Then reactors were placed in water baths to maintain a temperature of $37\text{ }^{\circ}\text{C}$. The stirrers of all the reactors were set to switch between on and off every 60 s at a speed of 60 rpm. The produced biogas flowed through 3 M NaOH solution to remove CO_2 and other impurities

and then passed through the gas tipping devices, which automatically recorded the biomethane production in each reactor. The biomethane yield in each reactor with seaweed feedstock was corrected by the biomethane yield from the blank group to eliminate the carryover effect of the inoculum. All the BMP assays were conducted in triplicate. The significance of differences between BMP means was analysed by multiple comparison test (Post Hoc) using the software IBM SPSS Statistics v25 at a significance level of $p = 0.05$.

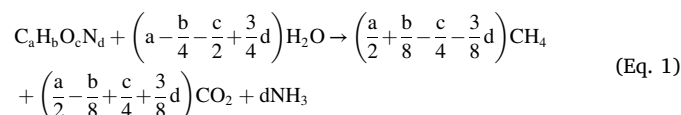
2.3. Analytical methods

The biological composition (the content of total solid (TS), VS, and ash) of the seaweed samples, inoculum, and anaerobic digestate was analysed according to the Standard Method 2540 G [52]. The elemental composition was analysed on the elemental analyser (Exeter Analytical, CE 440 Model). The major VFAs in the AD effluents were measured on a gas chromatography system (Agilent 7890B, USA) equipped with a flame ionization detector and the DB-FFAP column ($\Phi\text{ }0.32\text{ mm} \times 50\text{ m}$). More details of these analytical methods have been described in the previous publication by the authors [53].

To prepare the suspension of biochar (or graphene) for pH and electrical conductivity measurement, a sample of 1.0 g oven dried biochar (or 1.0 g oven dried graphene) was dispersed into 10.0 ml of deionized water. The suspension samples were made in triplicate. The pH of the suspensions was measured using a digital pH meter (Mettler Toledo FiveEasy F20). The electrical conductivity of the suspensions was measured by a multi-parameter meter (Portable Conductivity, Salinity and Temperature Instrument VWR CO310). The surface morphology of biochar was examined on the scanning electron microscope (SEM, Hitachi SU8010, Japan) operated at 200 kV. The nitrogen adsorption isotherm of biochar was obtained on a Micrometrics ASAP 2020 analyser and used to determine the specific surface area via the Brunauer-Emmett-Teller (BET) method. The average pore diameter (d) was calculated by $d = 4V/S_{\text{BET}}$, in which V was the total pore volume obtained at the last point of the isotherm and S_{BET} was the BET specific surface area. The crystallinity of biochar was evaluated based on the X-ray diffraction (XRD) pattern in the wide range of $5\text{--}90^{\circ}$ recorded by X'Pert PRO.

2.4. Kinetic modelling

The maximum theoretical biomethane potential of seaweed was calculated as per the Buswell Equation (Eq. (1)):



The biodegradability index (BI) was defined as the ratio of SMY to the maximum theoretical biomethane potential.

The modified Gompertz equation (Eq. (2)) was used to assess the process kinetics and predict the maximum biomethane yield (H_m , ml/g VS), the peak biomethane production rate (R_m , ml/g VS/d), and the lag-phase time (λ , d). The peak time of the fermentation process (T_m , d) was defined as per Eq. (3).

$$H = H_m \exp \left\{ - \exp \left[\frac{R_m e}{H_m} (\lambda - t) + 1 \right] \right\} \quad (\text{Eq. } 2)$$

$$T_m = \frac{H_m}{R_m e} + \lambda \quad (\text{Eq. } 3)$$

2.5. Energy calculations

The higher heating value (HHV) of the seaweed feedstock and the solid digestate was calculated according to the modified Dulong

Table 3
Characteristics of the seaweed feedstock and inoculum.

	<i>L. digitata</i>	<i>S. latissima</i>	Inoculum
<i>Proximate analysis</i>			
TS (wwt%)	9.5 ± 0.3	13.8 ± 0.1	2.4 ± 0.0
VS (wwt%)	7.6 ± 0.3	10.1 ± 0.1	1.3 ± 0.0
Ash (wwt%)	1.7 ± 0.0	3.6 ± 0.0	1.1 ± 0.0
Moisture (wwt%)	90.5 ± 0.3	86.2 ± 0.1	97.6 ± 0.0
VS/TS	0.80	0.73	0.54
<i>Ultimate analysis</i>			
C (% VS)	48.0 ± 0.2	46.1 ± 1.8	47.8 ± 0.3
H (% VS)	6.3 ± 0.0	5.9 ± 0.2	5.7 ± 0.0
N (% VS)	3.1 ± 0.0	2.9 ± 0.1	4.5 ± 0.0
O (% VS)	42.6 ± 0.2	45.1 ± 2.2	42.0 ± 0.3
C:N	15.5	15.9	10.6
<i>Energy content</i>			
HHV (kJ/g VS)	17.6	15.9	\
LHV (kJ/g VS)	15.9	14.3	\
Theoretical biomethane potential (ml/g VS)	455.8	419.4	\

Note: The results of ultimate analysis were converted to a VS basis from the raw data.

Formula (Eq. (4)) [54]:

$$\text{HHV (MJ/kg VS)} = 0.337 \times \text{C} + 1.419 \times (\text{H} - 0.125 \times \text{O}) + 0.023 \times \text{N} \quad (\text{Eq. 4})$$

The lower heating value (LHV) was converted from the HHV according to Eq. (5) [55]:

$$\text{LHV (MJ/kg VS)} = \text{HHV} - 0.212 \times \text{H} - 0.008 \times \text{O} \quad (\text{Eq. 5})$$

in both of which C, H, O, and N refer to the weight percentage of each element on a VS basis.

The standard Gibbs free energy at pH = 7 (ΔG^0) for chemical reactions was calculated from the free energy of formation (G_f^0) of products and reactants (Eq. (6)) [56].

$$\Delta G^0 = \sum G_f^0(\text{products}) - \sum G_f^0(\text{reactants}) \quad (\text{Eq. 6})$$

in which $\sum G_f^0(\text{products})$ is the sum of the G_f^0 of products and $\sum G_f^0(\text{reactants})$ is the sum of the G_f^0 of reactants. The free energies of formation (G_f^0) for the substances in this study were also adopted from Madigan et al. [56].

3. Results and discussion

3.1. Characteristics of graphene and biochar

The characteristics of seaweed samples and the inoculum are shown in Table 3. The theoretical biomethane potential of *L. digitata* was calculated as 455.8 ml/g VS and that of *S. Latissima* as 419.4 ml/g VS according to the Buswell Equation.

The characteristics of biochar are shown in Table 4 in comparison with those of graphene. The pH value of the biochar suspension was in the range of 8.95–9.22, while the pH value of the graphene suspension was in the range of 4.37–5.12. The specific surface area of biochar was 161.5 m²/g, equivalent to one third of the specific surface area of graphene (500.0 m²/g). The average pore diameter of biochar was 2.5 nm.

Table 4
Characteristics of biochar and graphene.

Material	Specific surface area (m ² /g)	Particle size (μm)	pH	Electrical conductivity (μS/cm)	CO ₂ /CH ₄ adsorption capacity at 0.1 MPa (ml/g)	Carbon content (TS %)
Biochar	161.5	75–500	8.95–9.22	251.7	47.6/22.5	87.8
Graphene	500.0 ^a	2 ^a	4.37–5.12	277.8	\	\

^a Data from product description of Sigma Aldrich.

The SEM images shown in Fig. S1 (included in the supplementary material) indicated the porous surface morphology of the biochar. The XRD pattern of the biochar powder (see Fig. S2 in the supplementary) showed two wide peaks at 2θ value of 25.5° and 43.3° corresponding to C (002) and C (100) diffraction planes, respectively, which are also typical diffraction peaks of graphene [57]. The diffraction peaks of biochar were wider, and the intensity of the peaks was lower compared to the diffraction peaks of graphene in the literature [57], which indicated that the crystallinity of biochar is lower than that of graphene.

3.2. Effect of graphene and biochar on biomethane production from *L. digitata*

3.2.1. Effect of graphene on biomethane production

Seaweed harvested in different seasons presents varied organic compositions, leading to variations in biomethane yield [9]. *L. digitata* harvested in May resulted in relatively low biomethane yields (ranging from 184.0 to 263.0 ml CH₄/g VS) among all the samples harvested over 12 months [14,25]. This was ascribed to the low C:N ratio (15.0 [14] – 16.9 [8]) and high polyphenols content (0.13% [14] – 0.18% [8]) in the May harvested *L. digitata* and high quantities of inhibitory hydrogen sulphide (more than 200 ppm) in the produced biogas [25].

Fig. 1. (a) shows biomethane yield from *L. digitata* with and without graphene addition. The BMP yield of *L. digitata* was 200.1 ml/g VS, corresponding to a BI of 44%. Such a low BI suggests that AD of raw *L. digitata* needs further optimisation to improve energy conversion efficiency. In an effort to stimulate DIET in AD, graphene and biochar were added to promote microbial interactions. As the dosage of graphene increased from 0.125 g (equivalent to an addition ratio of 1/16) to 0.250 g (equivalent to an addition ratio of 1/8), the BMP yield from *L. digitata* presented similar values to the control group with slight decreases ($p > 0.05$). This may be possibly due to the adsorption of biomethane on graphene [58,59]. The optimal graphene addition ratio of 1/4 led to the highest BMP yield of 248.8 ml/g VS, a significant increase of 24% ($p < 0.05$) compared to the control group. However, further increases in graphene addition ratio resulted in decreases in BMP yield. The lowest biomethane yield of 154.2 ml/g VS was observed at the graphene addition ratio of 2/1, which was 23% lower ($p < 0.05$) than that of the control group. Similar phenomenon was observed previously by Lin et al. [34,36,37], the results of which suggested that the optimal concentration of graphene for enhancing biomethane production from ethanol and glycine might be around 0.5–1.0 g/L. The adverse effect of excess graphene was ascribed to the microbial inhibition induced by high concentration of nanoscale particles. Tian et al. found that in contrast to the positive effect on short-term AD, long-term exposure of 0.12 g/L graphene in a digester treating sludge suppressed the growth of dominant species (such as *Methanosaeta*, *Lactococcus* and *Anaerolinea*) and affected the methanogenesis performance afterwards [35]. Palmieri et al. introduced three action modes (namely cutting, wrapping and trapping) between nano graphene oxide and microbes, in which the wrapping could inhibit or even kill the methanogens by causing membrane mechanical injury and oxidative stress [60]. Zhang et al. speculated that wrapping did not predominate until the concentration of graphene oxide reached 0.1 g/L in digestion of swine manure [61]. Dong et al. found that nano graphene oxide significantly inhibited the methanogenic process of wastewater sludge through inhibiting the relevant enzyme activity (coenzyme F420) [62]. The sharp edges of graphene

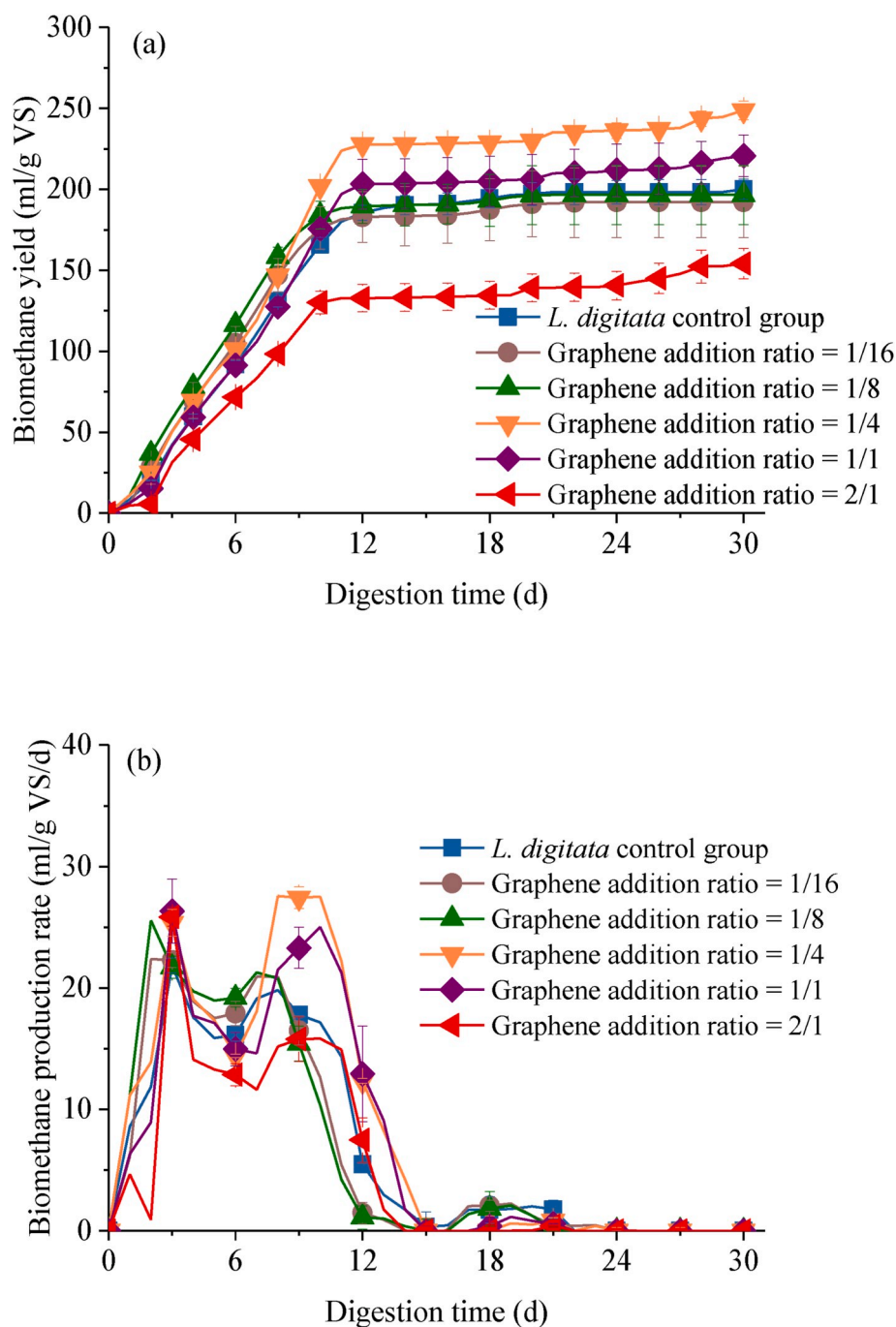


Fig. 1. Effects of graphene addition on (a) biomethane yield and (b) biomethane production rate in anaerobic digestion of *L. digitata*.

Table 5

Kinetic analysis of *L. digitata* digestion with different additions of graphene.

Graphene addition ratio	Experimental data			Kinetic model parameters				
	BMP (ml/g VS)	Peak production rate (ml/g VS/d)	BI (%)	H _m (ml/g VS)	R _m (ml/g/d)	λ (d)	T _m (d)	R ²
0	200.1 ± 6.3	21.8 ± 0.6	44	199.8 ± 1.1	22.1 ± 0.6	1.5 ± 0.1	4.8 ± 0.1	0.996
1/16	192.2 ± 22.0	22.4 ± 6.4	42	191.8 ± 1.0	24.1 ± 0.8	1.2 ± 0.1	4.1 ± 0.1	0.996
1/8	196.5 ± 18.4	25.6 ± 0.9	43	196.8 ± 1.0	25.5 ± 0.8	0.9 ± 0.1	3.8 ± 0.1	0.996
1/4	248.8 ± 5.7	27.5 ± 0.3	54	240.2 ± 2.4	26.2 ± 1.4	1.6 ± 0.3	5.0 ± 0.1	0.988
1/1	220.8 ± 12.8	26.3 ± 2.6	48	214.6 ± 2.0	23.6 ± 1.2	1.8 ± 0.2	5.2 ± 0.1	0.990
2/1	154.2 ± 9.5	25.8 ± 0.8	35	143.0 ± 1.5	17.0 ± 1.0	1.6 ± 0.3	4.7 ± 0.2	0.986

Note: Graphene addition ratio: the mass ratio of graphene to volatile solid (VS) in *L. digitata*; BMP: biomethane potential; BI: biodegradability index.

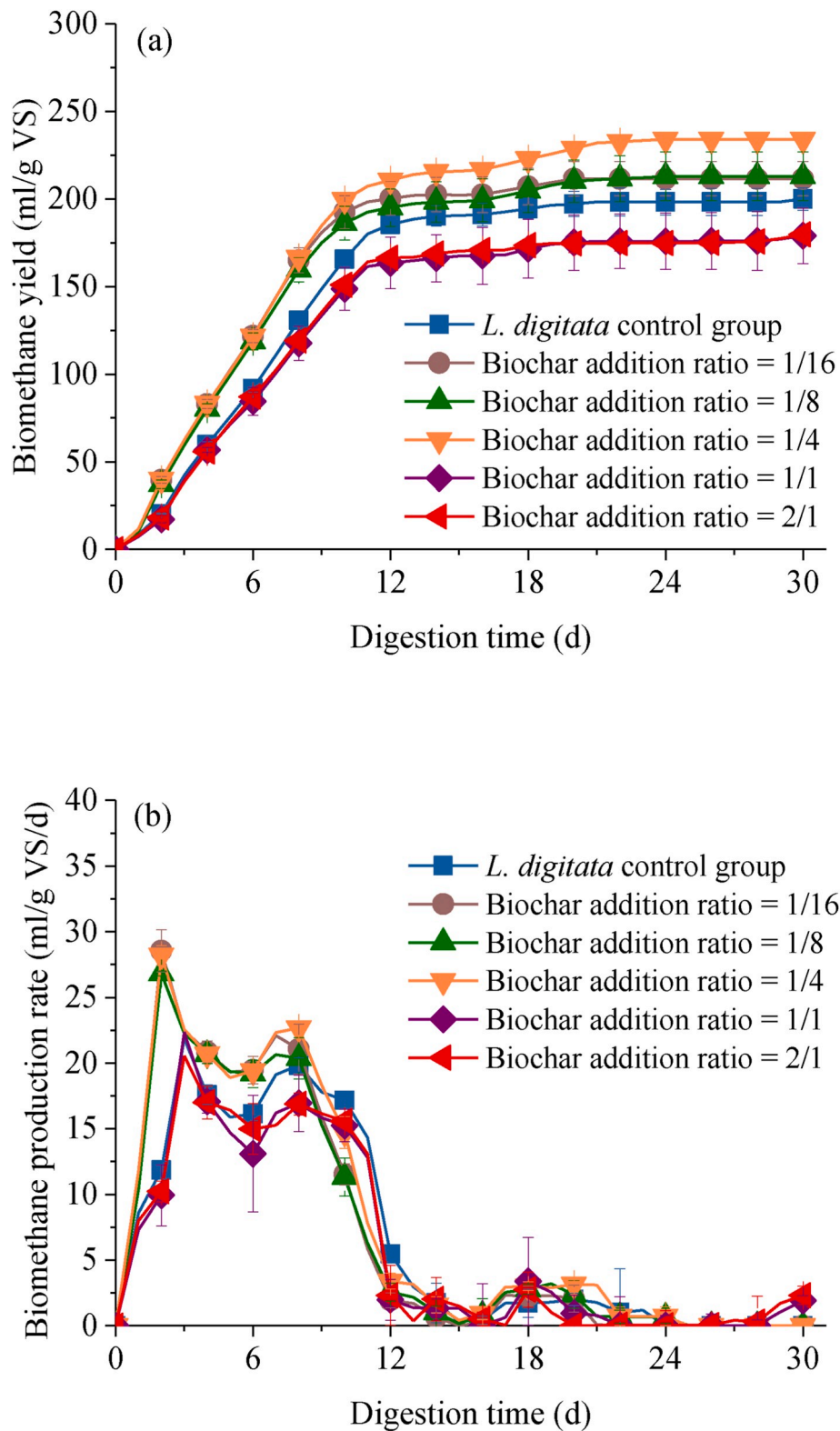


Fig. 2. Effects of biochar addition on (a) biomethane yield and (b) biomethane production rate in anaerobic digestion of *L. digitata*.

oxide nanosheets contributed to an increase in membrane pressure, which might damage the structure of the cell membrane, leading to discharge of intracellular materials such as RNA [62]. These studies indicate the concern of cytotoxicity of nanomaterials, which may be a limiting factor when applying nanomaterials in AD. However, the comprehensive toxicological mechanisms have not been clearly

addressed yet.

Fig. 1. (b) illustrates the effects of graphene on biomethane production rate from *L. digitata*. In the control group, the biomethane production rate reached a peak of 21.8 ml/g VS/d on the third day and showed a second peak value of 19.8 ml/g VS/d on the eighth day. The addition of graphene accelerated the production of biomethane.

Table 6
Kinetic analysis of *L. digitata* digestion with different additions of biochar.

Biochar addition ratio	Experimental data			Kinetic model parameters				
	BMP (ml/g VS)	Peak production rate (ml/g/d)	BI (%)	H _m (ml/g)	R _m (ml/g/d)	λ (d)	T _m (d)	R ²
0	200.1 ± 6.3	21.8 ± 0.6	44	199.8 ± 1.1	22.1 ± 0.6	1.5 ± 0.1	4.8 ± 0.1	0.996
1/16	211.5 ± 9.7	28.5 ± 1.6	46	211.2 ± 1.0	25.8 ± 0.7	0.8 ± 0.1	3.8 ± 0.1	0.996
1/8	212.9 ± 13.9	26.8 ± 0.2	47	211.0 ± 1.0	24.2 ± 0.7	0.8 ± 0.1	4.0 ± 0.1	0.996
1/4	234.0 ± 2.1	28.2 ± 0.8	51	232.1 ± 1.3	24.7 ± 0.7	0.7 ± 0.1	4.2 ± 0.1	0.996
1/1	180.0 ± 15.6	22.3 ± 0.7	39	176.8 ± 1.0	19.5 ± 0.6	1.3 ± 0.1	4.7 ± 0.1	0.996
2/1	179.7 ± 3.0	20.5 ± 0.9	39	176.8 ± 1.0	20.3 ± 0.6	1.4 ± 0.1	4.6 ± 0.1	0.996

Note: Biochar addition ratio: the mass ratio of biochar to volatile solid (VS) in *L. digitata*; BMP: biomethane potential; BI: biodegradability index.

Compared to the control group, a maximum increase of 26% ($p < 0.05$) was obtained at a graphene addition ratio of 1/4. Correspondingly, the production rate achieved the first peak value of 25.3 ml/g VS/d on the second day and the second peak value of 27.5 ml/g VS/d on the ninth day at the addition ratio of 1/4. Further increasing the addition ratio to 2/1 decreased the peak production rate to 25.8 ml/g VS/d and delayed its occurrence to the third day. This indicated that excessive addition of graphene resulted in a reduction of biomethane production rate and an increase in the lag phase time. The kinetic parameters estimated by fitting the Gompertz model are shown in Table 5. The modelling results of biomethane potential and biomethane production rate accurately matched the experimental results with coefficients of determination over 0.986. The predicted values suggested that both biomethane yield and biomethane production rate were maximized as the addition ratio of graphene reached 1/4 and decreased with further increases in the graphene addition ratio. The predicted lag-phase time λ and the peak time T_m achieved the lowest values at the graphene addition ratio of 1/8.

3.2.2. Effect of biochar on biomethane production

The biomethane yield and biomethane production rate from *L. digitata* with different dosages of biochar addition are shown in Fig. 2. Fig. 2. (a) indicated that biomethane yield was enhanced with biochar added at ratios ranging from 1/16 to 1/4. Fig. 2. (b) showed that the peak production rate was achieved one day earlier with biochar addition compared to the control group. The biochar addition at an optimal ratio of 1/4 led to the highest biomethane yield of 234.0 ml/g VS and a relatively high peak production rate of 28.2 ml/g VS/d, corresponding to a 17% increase ($p < 0.05$) in biomethane yield and a 29% increase ($p < 0.05$) in peak production rate compared to the control group. The biomethane yield with biochar added at the optimal ratio of 1/4 exhibited no significant difference ($p > 0.05$) to the biomethane yield with graphene added at the same ratio, which may suggest an opportunity for using biochar as a cost-effective replacement of graphene to enhance biomethane yield through stimulating DIET. It is notable that biomethane yield was inhibited as the biochar addition ratio increased beyond 1/1. The lowest biomethane yield of 179.7 ml/g VS was obtained at a biochar addition ratio of 2/1, a 10% decrease ($p < 0.05$) compared to that of the control group. Similarly, significant decreases in biomethane yield were observed by Li et al. [63] when biochar was added at 3.9 g/g TS of sludge and by Zhang et al. [64] when biochar was added at 0.4 g/g TS of sewage sludge. The authors attributed the inhibition effect to the nonselective adsorption of nutrients and useful metabolites and the destruction of the microorganism diversity caused by biochar [63,64]. As shown in Table 6, the predicted biomethane yield H_m agreed well with the experimental data with coefficients of determination of 0.996. The predicted peak production rate R_m showed slight differences to the experimental data. The predicted lag-phase time λ and the peak time T_m presented lower values when the biochar addition ratio was in the range of 1/16 to 1/4.

3.2.3. Profiles of VFAs

The variation of major VFAs during the digestion of *L. digitata* in the

control group is shown in Fig. 3. (a). The VFAs accumulated to the highest level of 1346.7 mg/L in four days. Acetic acid and propionic acid were dominant compounds, which accounted for 70% and 17% of the total VFAs on the fourth day, respectively. From the sixth to the ninth day, the total amount of VFAs decreased from 1101.3 to 355.9 mg/L. Thereafter, the amount of VFAs gradually decreased to 38.2 mg/L.

As shown in Fig. 3. (b), the graphene addition at a ratio of 1/4 accelerated the accumulation of VFAs at the start-up. Graphene enhanced the total VFAs concentration on the second day to 1267.5 mg/L, which was 31% higher than that of the control group. On the fourth day, the total VFAs reached the maximum concentration of 1416.9 mg/L, in which acetic acid and propionic acid accounted for 74% and 15%, respectively. This indicated that graphene addition facilitated the production of acetic acid.

As shown in Fig. 3 (c), with biochar added at a ratio of 1/4, the concentration of VFAs achieved the maximum value of 1389.1 mg/L on the fourth day, in which the shares of acetic acid and propionic acid were 70% and 15%, respectively. The addition of biochar did not change the composition of the major VFAs significantly compared to that of the control group. The concentration of total VFAs dropped to 253.9 mg/L on the ninth day. The addition of biochar presented no significant impact ($p > 0.05$) on the total VFAs amount during the digestion of *L. digitata*.

The concentration of butyric acid during AD is specified in Fig. 4. (a). In the *L. digitata* control group, butyric acid accumulated slowly to 84.0 mg/L in 21 days. Then it was degraded slowly to 38.2 mg/L after 30 days. When graphene or biochar was added at the addition ratio of 1/4, the accumulation of butyric acid was significantly accelerated at the start-up. The butyric acid accumulated to the peak level of 120.2 mg/L on the ninth day with graphene addition, while it accumulated to the peak level of 94.9 mg/L on the fourth day with biochar addition. The addition of graphene and biochar accelerated acidogenesis and acetogenesis. In a previous study, Wang et al. concluded that biochar accelerated the conversion of butyrate to acetate by promoting DIET [65].

The concentration of propionic acid during AD is specified in Fig. 4. (b). Propionic acid in the control group reached 239.6 mg/L on the sixth day, then was gradually consumed in AD. With graphene addition at a ratio of 1/4, propionic acid reached the highest concentration of 216.4 mg/L on the fourth day and decreased rapidly to 10.0 mg/L on the sixth day. With addition of biochar at a ratio of 1/4, the highest concentration of propionic acid 211.9 mg/L occurred on the fourth day. Thereafter, propionic acid was degraded gradually to zero on the ninth day. The anaerobically oxidation of butyrate and propionate to acetate through MIET pathway are described in R1 and R2. The energy barrier to oxidize propionate to acetate ($\Delta G^0 = +71.6$ kJ/mol) is much higher as compared to that for butyrate ($\Delta G^0 = +48.3$ kJ/mol), which agrees with the results of Wang et al. [65,66] and Amani et al. [67]. Therefore, the accumulation of propionic acid in the control group led to the slower acetogenic rate of propionic acid, consequently, a lower biomethane production rate. The addition of graphene and biochar alleviated the accumulation of propionic acid and promoted its syntrophic oxidation via DIET enhancement. Wang et al. explained that the VFA oxidizing

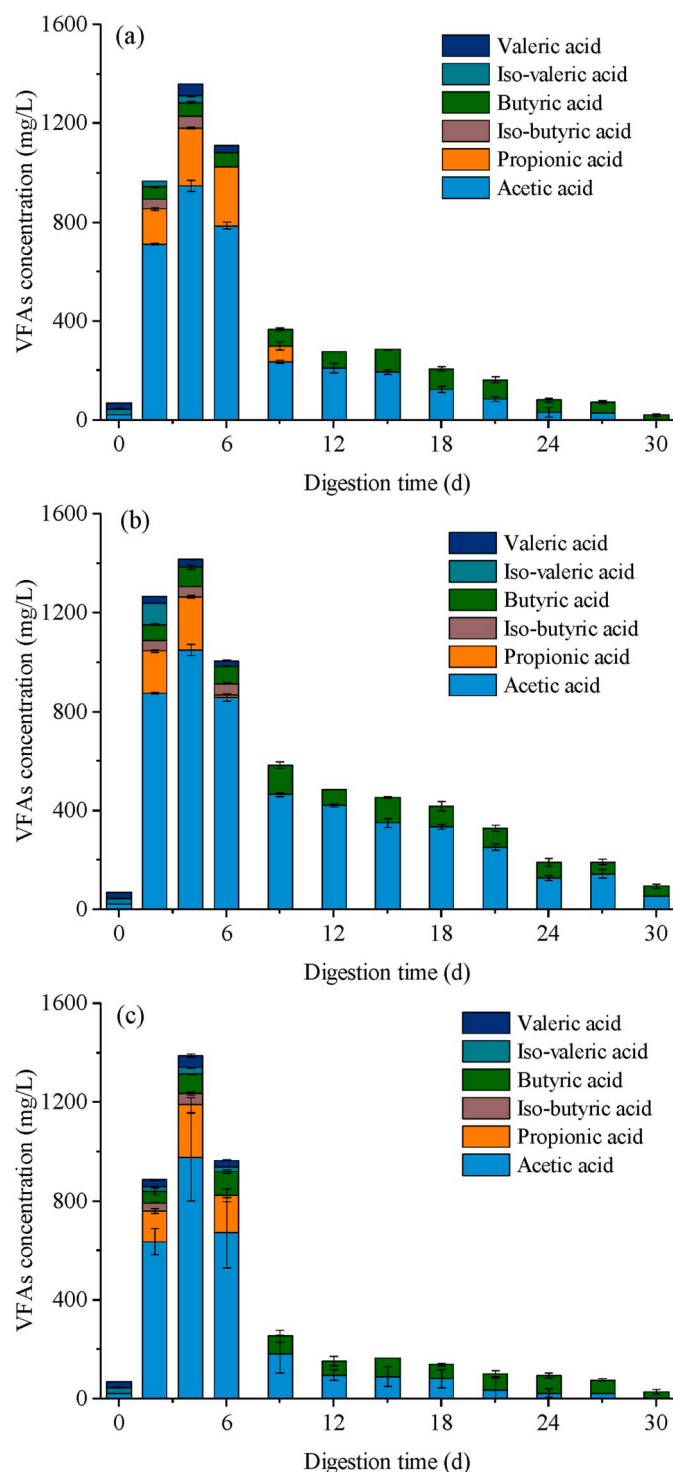
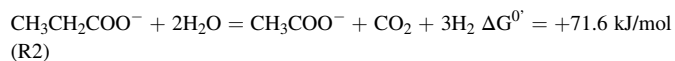


Fig. 3. Variations of volatile fatty acids (VFAs) during anaerobic digestion of *L. digitata*: (a) control group, (b) with graphene added at the optimal addition ratio of 1/4, and (c) with biochar added at the optimal addition ratio of 1/4.

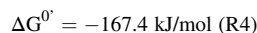
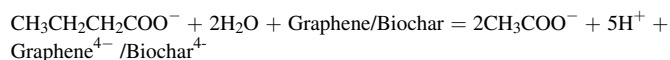
bacteria oxidized butyrate/propionate to acetate using graphene/biochar as the temporary electron acceptor in the inactive metabolism of methanogenic archaea [65]. The oxidation of butyrate and propionate through DIET pathway could be simulated as R3 and R4 [68]. The ΔG° for butyrate oxidation through DIET pathway was -111.0 kJ/mol and ΔG° for propionate oxidation through DIET pathway was -167.4 kJ/mol. It indicates the oxidation of propionate was more thermodynamically favourable than the oxidation of butyrate

in the presence of graphene/biochar.

MIET pathway:



DIET pathway:



The initial pH values of the *L. digitata* control group, optimal graphene group, and optimal biochar group in AD were measured as 8.66 ± 0.01 , 8.69 ± 0.02 and 8.70 ± 0.02 , respectively. Although the pH values of the graphene (4.37–5.12) and biochar (8.95–9.22) suspensions were different, the end pH values of the control group (7.67 ± 0.05), the optimal graphene group (7.69 ± 0.07), and the optimal biochar group (7.61 ± 0.06) were similar ($p > 0.05$). Therefore, it was conceivable that the pH buffering capacity of biochar was not the decisive factor affecting biomethane production from *L. digitata*.

3.3. Effect of biochar on biomethane production from *S. latissima*

3.3.1. Effect of biochar on biomethane production

The effects of biochar addition on the biomethane production from *S. latissima* are illustrated in Fig. 5. The biomethane yield from *S. latissima* control group was 265.4 ml/g VS, equivalent to a BI of 63%. The addition of biochar at lower ratios ranging from 1/16 to 1/4 did not present a significant influence ($p > 0.05$) on the biomethane yield. At the addition ratio of 1/1, biochar significantly ($p < 0.05$) enhanced biomethane yield to 308.8 ml/g VS, equivalent to a BI of 74%. Further increasing the biochar addition ratio to 2/1 still had a positive effect on improving the cumulative biomethane yield, but made little significant enhancement (especially considering twice the addition of biochar) as compared to the addition at a ratio of 1/1. The recommended pragmatic biochar addition ratio of 1/1 led to a 16% increase in the biomethane yield compared to the control group. The peak production rate was 29.0 ml/g VS/d in the control group, and it significantly ($p < 0.05$) increased to 37.6 ml/g VS/d with the addition of biochar at a ratio of 1/1. The kinetic modelling predicted H_m and R_m (as shown in Table 7) showed close correlation with experimental data, confirming the enhancement by biochar addition. However, the predicted values of λ and T_m indicated that biochar addition had no significant influence on the lag-phase time and the peak time.

3.3.2. Profiles of VFAs

Fig. 6. (a) presents the VFAs concentration during digestion of *S. latissima*. The total concentration of VFAs increased quickly at the start-up and reached the highest value of 2362.5 mg/L on the fourth day, with acetic acid and propionic acid accounting for 71% and 18% of the total VFAs, respectively. The VFAs concentration dropped from 1989.7 mg/L on the sixth day to 637.8 mg/L on the ninth day. Consequently, the biomethane production rate increased from 18.6 to 28.7 ml/g VS/d. The VFAs concentration further decreased to 80.3 mg/L on the twelfth day and thereafter fluctuated at a low level to the final day. As shown in Fig. 6. (b), with biochar added at a ratio of 1/1, the highest VFAs concentration of 2567.1 mg/L was achieved on the fourth day, in which acetic and propionic acid accounted for 70% and 20%, respectively. The highest concentration of acetic acid was 1797.9 mg/L and the highest

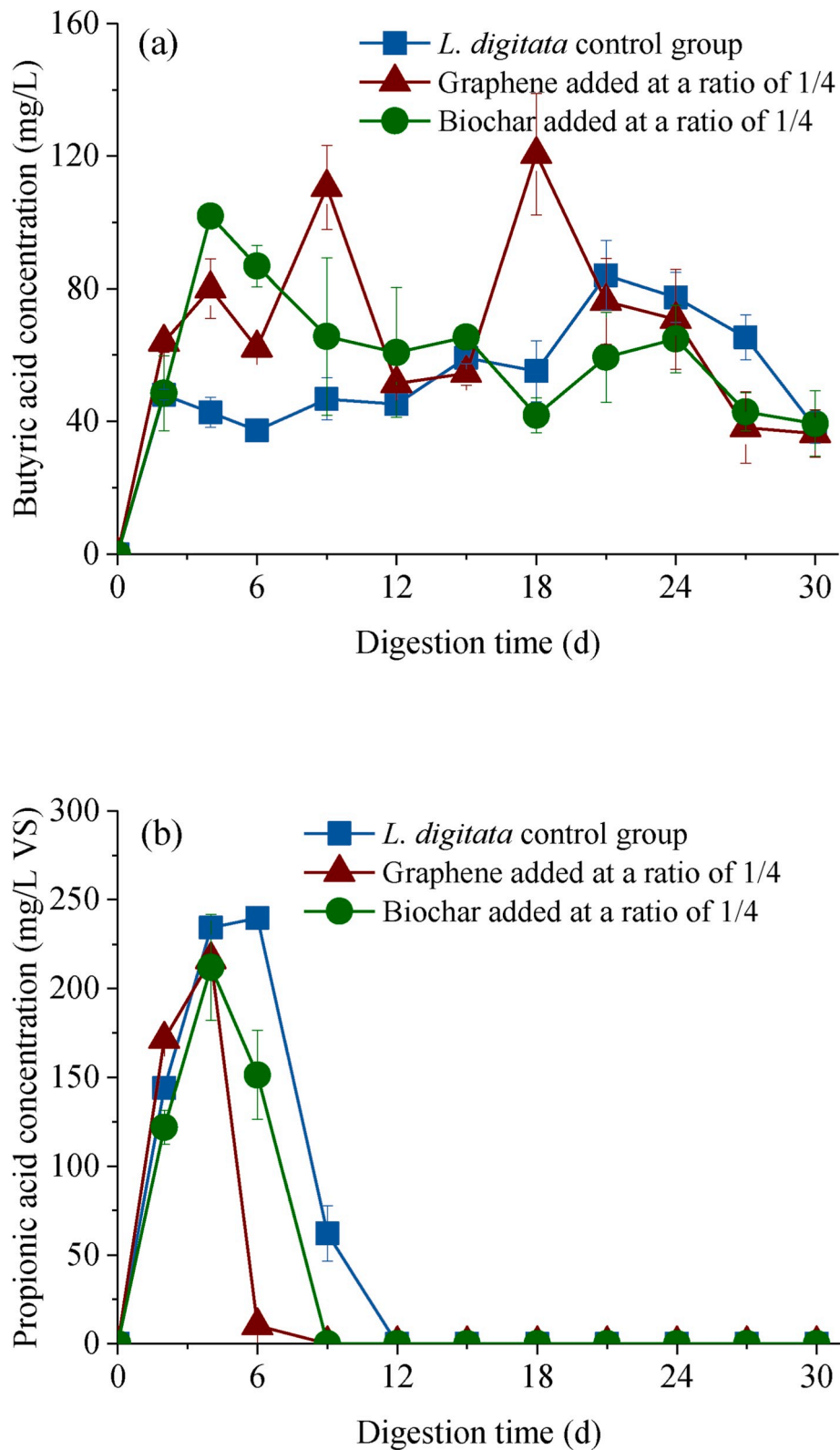


Fig. 4. Variations of (a) butyric acid and (b) propionic acid during anaerobic digestion of *L. digitata* with and without carbon additives.

concentration of propionic acid was 503.5 mg/L. The concentrations of both the acetic and propionic acids were well below their inhibitive concentrations which were reported to be 2500 mg/L and 800 mg/L, respectively [69]. The VFAs concentration remained at a high level of 2531.1 mg/L on the sixth day and then dramatically dropped to 911.0 mg/L on the ninth day. The rapid consumption of VFAs led to the second

peak of biomethane production rate on the ninth day as shown in Fig. 5 (b). The profiles of propionic and butyric acids are displayed in Fig. 7. Biochar addition made no significant influence on butyric acid accumulation and degradation. However, it accelerated both the accumulation and the degradation of propionic acid, which was beneficial for biomethane production.

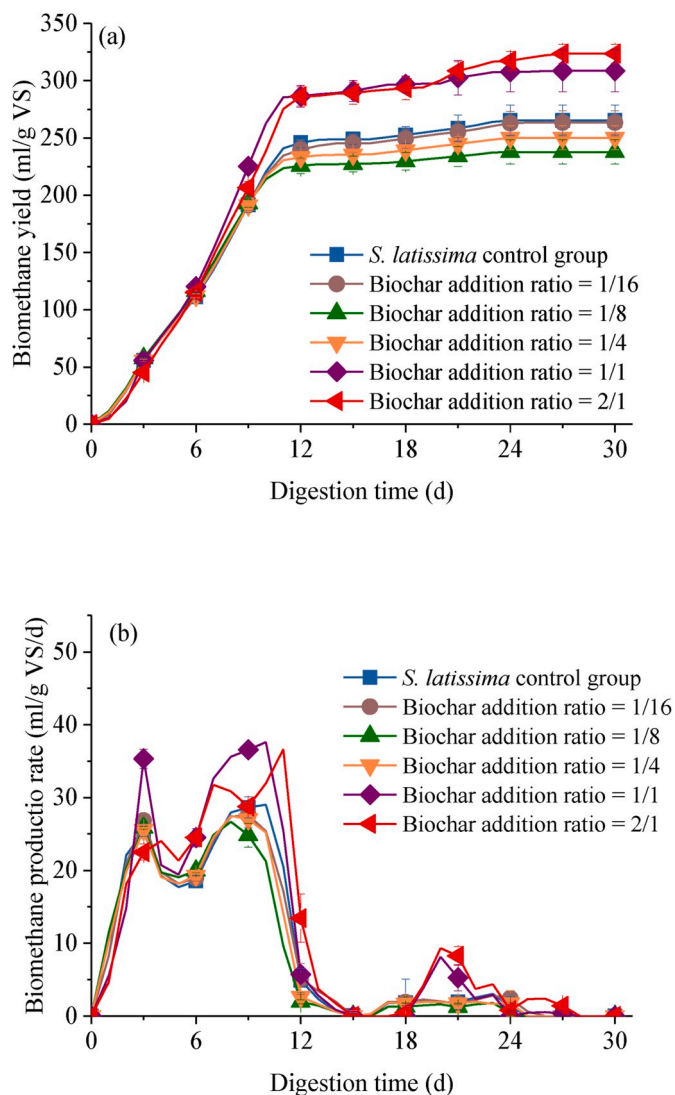


Fig. 5. Effects of biochar addition on (a) biomethane yield and (b) biomethane production rate in anaerobic digestion of *S. latissima*.

The initial pH values of the *S. latissima* control group and the recommended biochar group were 8.64 ± 0.01 and 8.65 ± 0.01 , respectively. The end pH values of the control group and the recommended biochar group were 7.64 ± 0.07 and 7.68 ± 0.06 , respectively. The pH buffering capacity of biochar did not present its influence on AD of *S. latissima*. Similar phenomenon was observed by Sunyoto et al. [70].

3.3.3. Potential mechanisms of biochar function in AD

Table 8 provides a brief review of biochar application in AD, indicating that biochars derived from various biomass are capable of

Table 7

Kinetic analysis of *S. latissima* digestion with different additions of biochar.

Biochar addition ratio	Experimental data			Kinetic model parameters				
	BMP (ml/g VS)	Peak production rate (ml/g/d)	BI (%)	H_m (ml/g)	R_m (ml/g/d)	λ (d)	T_m (d)	R^2
0	265.4 ± 13.5	29.0 ± 1.1	63	265.0 ± 2.2	28.3 ± 1.2	1.6 ± 0.2	5.0 ± 0.1	0.992
1/16	263.5 ± 10.3	27.6 ± 1.7	63	261.9 ± 1.9	27.7 ± 1.1	1.5 ± 0.2	5.0 ± 0.1	0.994
1/8	237.7 ± 10.6	26.7 ± 0.9	57	237.5 ± 1.6	28.1 ± 1.1	1.4 ± 0.2	4.5 ± 0.1	0.994
1/4	250.2 ± 10.5	27.0 ± 0.6	60	249.4 ± 1.9	27.8 ± 1.2	1.5 ± 0.2	4.8 ± 0.1	0.993
1/1	308.8 ± 18.4	37.6 ± 0.5	74	308.1 ± 2.6	36.1 ± 1.7	2.2 ± 0.2	5.4 ± 0.1	0.992
2/1	323.6 ± 8.2	36.6 ± 0.3	77	317.6 ± 2.8	32.6 ± 1.4	2.2 ± 0.2	5.8 ± 0.1	0.992

Note: Biochar addition ratio: the mass ratio of biochar to volatile solid (VS) in *S. latissima*; BMP: biomethane potential; BI: biodegradability index.

enhancing biomethane production by 8%–72%. However, the optimal addition ratio varies significantly depending on the biochar properties and feedstock characteristics. In this study, the biomethane yield from both *L. digitata* and *S. latissima* were enhanced with suitable biochar additions. However, excessive addition of biochar hampered AD performances. The effects of biochar on AD of straw and cow manure were investigated by Shen et al. [71], whose results showed that when biochar doses were too high, cumulative methane yields decreased in response to the shift of dominant archaea from *Methanoseta* to *Methanosarcina*. The adverse effects of excessive biochar were also observed in AD of food waste [72,73], hydrogen fermentation of municipal solid waste [74], and AD of citrus peel waste [75]. The decreased methane yield may be related to a decrease in soluble organic substrate availability due to the strong adsorption of biochar or the destruction of the microorganism diversity induced by biochar [62,76].

In this study, biochar addition increased biomethane yield from *L. digitata* by 17% which is comparable to the enhancement effect of graphene at the same addition ratio, though biochar and graphene differ in their properties. There are still arguments on how biochar properties relate to DIET promotion mechanisms. Some researchers reported that the excellent conductivity of biochar rather than the functional quinone moieties is the key property to promote DIET [77,78]. However, it has also been reported more recently that the bulk conductivity of biochar does not play the decisive role in enhancing AD. Carbon cloth and granular activated carbon could induce similar enhancement in AD performance, even though their conductivities were different by several orders of magnitude [79]. Barua et al. speculated that there may be a critical value for conductivity promoting AD, beyond which conductivity is no longer a limiting factor [80]. Shanmugam et al. observed that in the AD of glucose and aqueous phase bio-oil, biochar increased biomethane yield by 72%; while granular activated carbon increased the yield by 40% [81]. An explanation was that the redox-active moieties on biochar promoted the electron transfer between fermentative bacteria and methanogens [81]. Zhang et al. [82] also reported that the electron transfer through the biochar depends on the charging and discharging cycles of the surface functional groups. Sun et al. [41] revealed that kinetically preferred electron transfer by carbon matrices over the surface quinone groups of biochar forms at pyrolysis temperatures higher than 700 °C.

Other surface characteristics also play important roles in facilitating the performance of AD, such as specific surface area, porosity, surface functional groups, and alkalinity, which are associated with the adsorption of substrate induced inhibitors, the colonisation of microbial cells, and the pH buffering capacity. On one hand, both the larger specific surface area and smaller particle size of graphene facilitate improved adsorption capacity, which benefits the adsorption of inhibitors and biomethane production. Kizito et al. reported that biochars exhibited a decrease in NH_3 adsorption with an increase in the particle size [83], but the specific surface area may not be the predominant factor in biochar adsorption [83,84]. On the other hand, adsorption by graphene and biochar is not selective; hence, it is possible that some of the nutrients or useful metabolites are adsorbed, which may lead to a

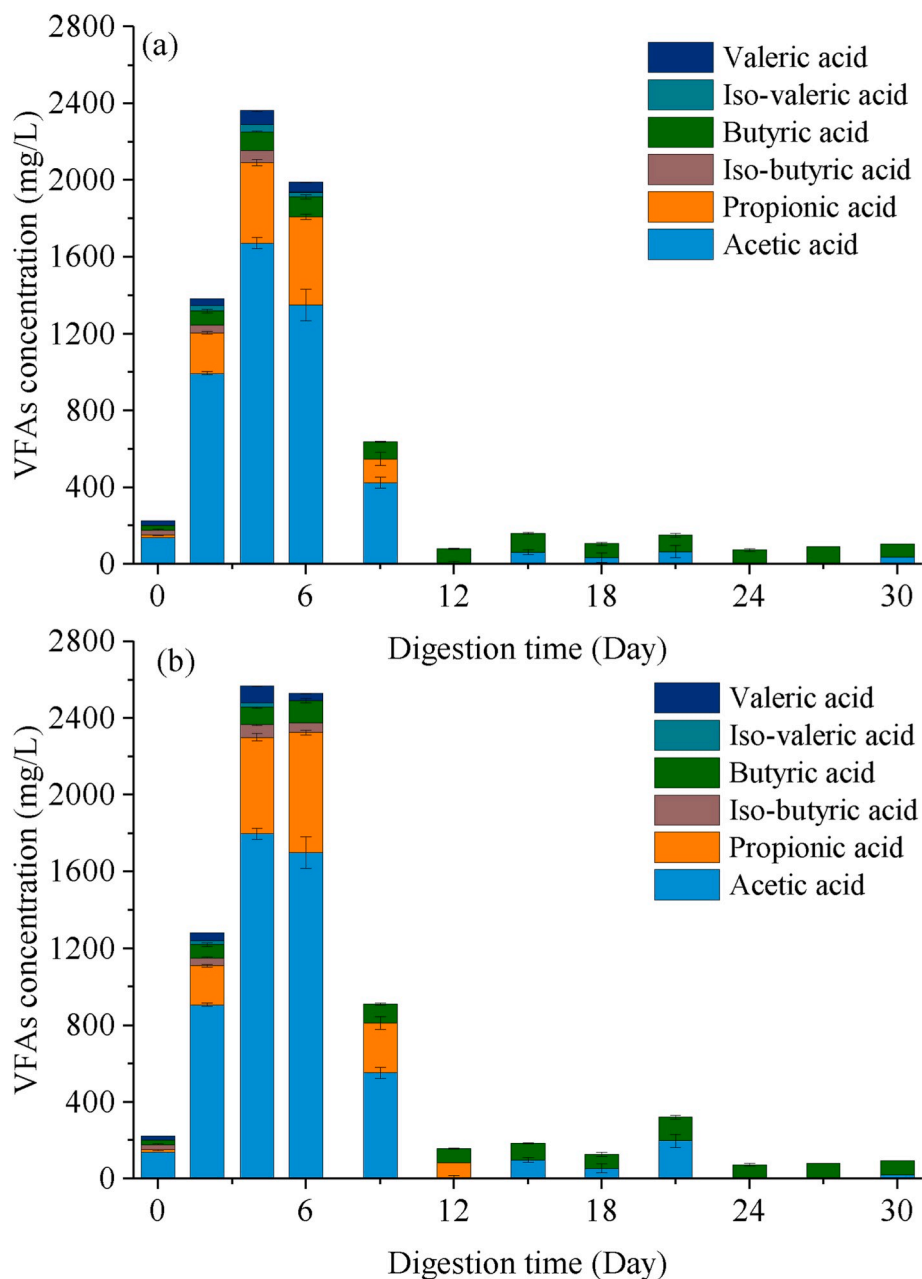


Fig. 6. Variations of volatile fatty acids (VFAs) during anaerobic digestion of *S. latissima*: (a) control group, and (b) with biochar added at the recommended addition ratio of 1/1.

negative effect on AD [85]. The nano size of graphene may also cause negative effects on AD by leading to cytotoxicity inhibition or difficulties for immobilization of microbial cells. In a study by Lü et al. [86], the adsorption of NH_3 on biochar with particle sizes ranging from 2.5 to 5 mm, 0.5–1 mm and 75–150 μm reduced the lag-phase time by 23.9%, 23.8%, and 5.9% and increased the CH_4 production rate by 47.1%, 23.5%, and 44.1%, respectively; it is suggested that an appropriate size of biochar particles should be selected to facilitate the colonisation of microbial cells. The interactive effects of these properties on the influence of biochar on AD are not fully understood as of yet. More knowledge on the optimal range of biochar properties is required for the selective production of biochar with tailored properties for AD

application.

3.4. Perspective on a cascading circular AD-Py system

3.4.1. Mass and energy balance of individual AD and Py system

The mass and energy balance of a conventional AD system were calculated based on the BMP results in section 3.2.2 (200.1 ml CH_4/g VS of *L. digitata* in the control group), characteristics of the digestate samples displayed in Table 9, and the following assumptions:

- (1) The mesophilic AD system is fed with wet *L. digitata*. The mass and energy calculations are based on per tonne of *L. digitata*

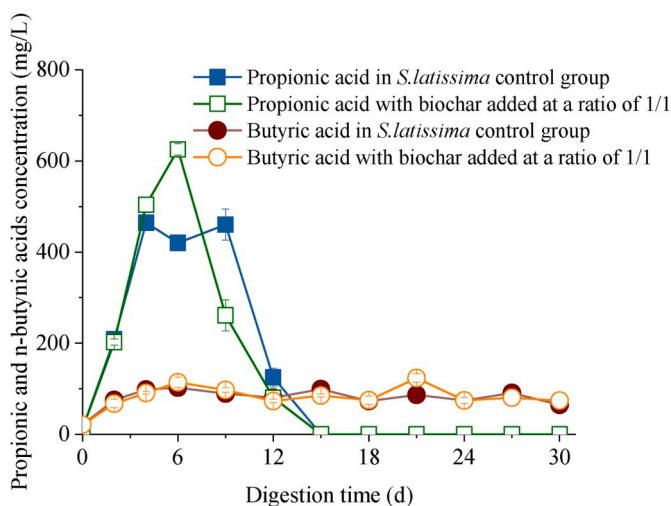


Fig. 7. Variations of butyric and propionic acids during anaerobic digestion of *S. latissima* with and without biochar addition.

(wwt) processed. The concentration of biomethane and carbon dioxide in the biogas are 60% and 40%, respectively. The electricity demand in the AD system is assumed as 10 kWh/t feedstock [92]. The heat demand for maintaining the temperature in the digester is calculated as per Eq. (7) [93]:

$$H_{IN AD} = C_p \times m_{LD} \times (T_{AD} - T_a) \tag{Eq. 7}$$

in which C_p is the specific heat capacity of water; m_{LD} is the weight of wet *L. digitata*; and $(T_{AD} - T_a)$ is the difference between the temperature inside the digester (37 °C) and the average ambient temperature (15 °C).

- (2) The digestate is separated into liquid digestate and wet solid digestate by decanter centrifuge. The majority of the non-degraded components in the digestate remains in the wet solid digestate after segregation, so the energy value of the liquid digestate is neglected [94]. The moisture content in the wet solid digestate is 70% [95]. The electricity consumption for digestate segregation is 3.5 kWh/t fresh digestate [96].
- (3) The energy value of biomethane refers to its LHV of 35.9 MJ/m³. The energy value of carbon dioxide is considered as zero.
- (4) The electricity and heat consumption for running the system is converted into primary energy consumption in a European

Table 8
Comparison of biochar application in batch anaerobic digestion (AD).

Biochar source	Pyrolysis condition	AD feedstock	AD temperature	Optimal addition ratio of biochar to feedstock	Effect on AD performance	Highlighted biochar properties	Reference
Wheat straw; Fruitwood; Chicken manure	350, 450, 550 °C; residence 2 h	Chicken manure	35 °C	5% TS	Fruitwood biochar derived at 550 °C increased the methane yield by 69%.	Specific surface area and ammonia nitrogen reduction capacity.	[87]
Wood; Coconut shell; Rice husk	450 °C	Citrus peel waste	35 °C	100% TS	Methane yield increased by 13%.	Colonisation and immobilization of microbes; surface structure.	[75]
Pine; White oak pellets	600–900 °C	Sewage sludge	37 °C; 55 °C	220%–249% TS	Methane yield increased by 8–10% under mesophilic condition and increased by 3% under thermophilic condition.	High aromaticity; cation exchange capacity; alkalinity.	[88]
Canola meal; Switch grass; Ashe juniper	400, 500, 600, 700, 900 °C	Glucose and aqueous phase of algae liquefaction	37 °C	1000% COD	Ashe juniper biochar derived at 400 °C increased the methane yield by 71%. Switch grass biochar derived at 500 °C increased the methane yield by 72%.	Electrical conductivity; redox active moieties; adsorption capacity.	[81]
Grass <i>Ampelodesmos mauritanicus</i>	450, 500, 550 °C	Cow manure and food waste digestate	37 °C	90% TS	Biogas production is faster and higher with biochar produced at higher temperatures.	Not specified.	[89]
Rice husk; Shrub; Peanut shell; Straw; Sawdust; Coconut shell; Tar	600 °C	Straw and cow manure	38 °C	25% TS	Methane yield increased by 13% with coconut shell biochar. Excess biochar (50% TS) inhibited AD.	A combination of pore structures, specific surface areas, surface functional group, and element distributions.	[71]
Macadamia nut shells	350, 500 °C; residence 2 h	Food waste	Room temperature	528% COD	COD removal efficiency increased by 15%.	Porosity	[90]
Pine	800 °C; residence 8 h	Oil	35 °C; 55 °C	333% VS	Methane production increased by 33% in granular biochar amended mesophilic digesters. Methane production increased by 13% in powdered biochar amended thermophilic digesters.	DIET	[91]
Waste wood	700 °C; residence 1 h	<i>L. digitata</i>	37 °C	25% VS	Methane yield increased by 17%. Maximum methane production rate increased by 29%.	DIET	This study
Waste wood	700 °C; residence 1 h	<i>S. latissima</i>	37 °C	100% VS	Methane yield increased by 16%. Maximum methane production rate increased by 30%.	DIET	This study

Table 9

Characteristics of the digestates from anaerobic digestion of *L. digitata* with and without biochar addition.

	Digestate from <i>L. digitata</i> control group	Digestate from <i>L. digitata</i> with biochar added at a ratio of 1/4
<i>Proximate analysis</i>		
TS (wwt%)	2.1 ± 0.3	2.2 ± 0.0
VS (wwt%)	1.2 ± 0.3	1.3 ± 0.0
Ash (wwt%)	1.0 ± 0.0	1.0 ± 0.0
Moisture (wwt%)	97.9 ± 0.3	97.6 ± 0.0
VS/TS	0.57	0.59
<i>Ultimate analysis</i>		
C (% VS)	49.0 ± 0.1	56.7 ± 0.7
H (% VS)	5.6 ± 0.0	5.3 ± 0.1
N (% VS)	4.3 ± 0.1	3.2 ± 0.2
O (% VS)	41.1 ± 0.0	34.7 ± 1.0
C:N	11.4	17.7
<i>Energy content</i>		
HHV (kJ/g VS)	17.3	20.6
LHV (kJ/g VS)	15.8	19.2

Note: The results of ultimate analysis were converted to a VS basis from the raw data.

context with primary energy conversion factors of 2.3 and 1.1 for electricity and heat, respectively [97].

- (5) The energy output of the AD system refers to the energy value of produced biomethane. The net energy gain is defined as the difference between the energy output and the primary energy consumption. The AD process efficiency is defined as Eq. (8).

Table S2 in the supplementary material presents the detailed calculations of mass and energy balance. Fig. 8 shows the mass and energy balance of the conventional AD system. The biomethane yield from 1.000 t wet *L. digitata* processed is calculated as 15.208 m³ and the corresponding carbon dioxide yield is 10.138 m³. In the segregation process, 0.213 t wet solid digestate and 0.756 t liquid digestate are obtained. The energy value of the processed *L. digitata* is 1208.4 MJ. In the anaerobic digester, 546.0 MJ of energy is converted into the LHV of biomethane, 672.4 MJ of energy remains in the wet solid digestate. The electricity consumption in the AD system is 36.0 MJ, equivalent to 7% of the energy output in biomethane, which is consistent with the literature data of 7% [98] and 9% [99,100]. The heat consumption in the AD system is 92.0 MJ, equivalent to 17% of the energy output in biomethane, which is higher than the literature data ranging from 7% [100], 8% [98], to 11% [99]. The higher ratio of heat demand was ascribed to the higher moisture content in *L. digitata* and lower biomethane production compared to other feedstocks. Dave et al. also obtained a high heat consumption of 13% of total energy output in biomethane when using *L. digitata* as feedstock [101]. The electricity consumed for digestate segregation is 12.2 MJ. The total primary energy consumption of the AD system is 223.3 MJ. Therefore, the net energy gain of processing 1.000 t wet *L. digitata* is 322.7 MJ. The energy output of this individual AD system is 546.0 MJ, resulting in a process efficiency of 38.1%. The relatively low process efficiency in this study is due to the low degradability of *L. digitata* harvested in May. Use of renewable energy would reduce the primary energy factor of electricity from 2.3 to 1.0 and generate higher process efficiency. Of more relevance to this analysis however is the relativity between AD and the AD-PY system.

The individual Py system is fed with forest residue which is not suitable for biodegradation in AD due to its rigid lignocellulosic struc-

$$\eta_{AD} = \frac{\text{Energy value of biomethane}}{\text{Energy value of the input } L.\text{digitata} + \text{Primary energy consumption to run the system}} \quad (\text{Eq. 8})$$

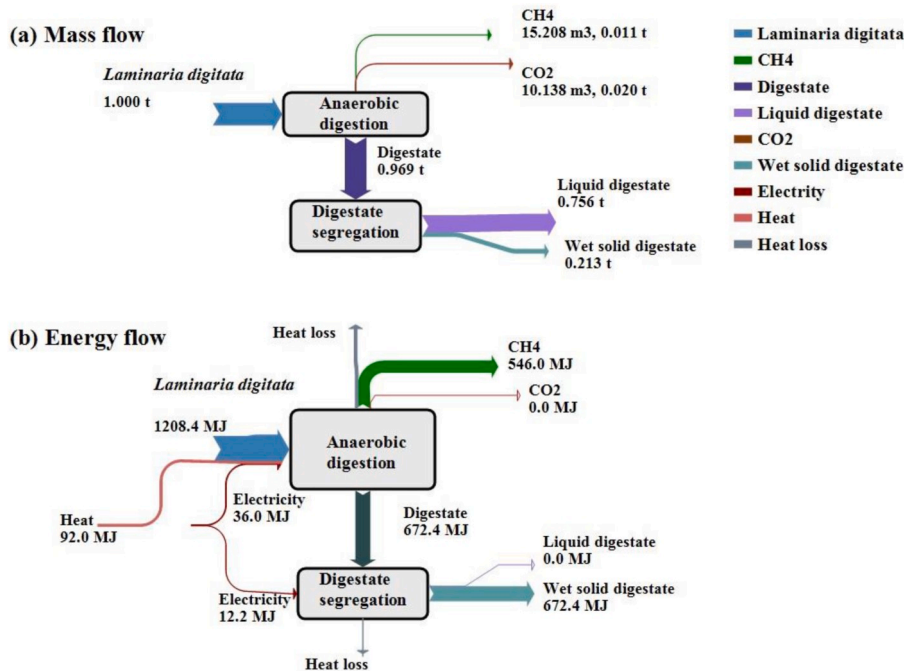
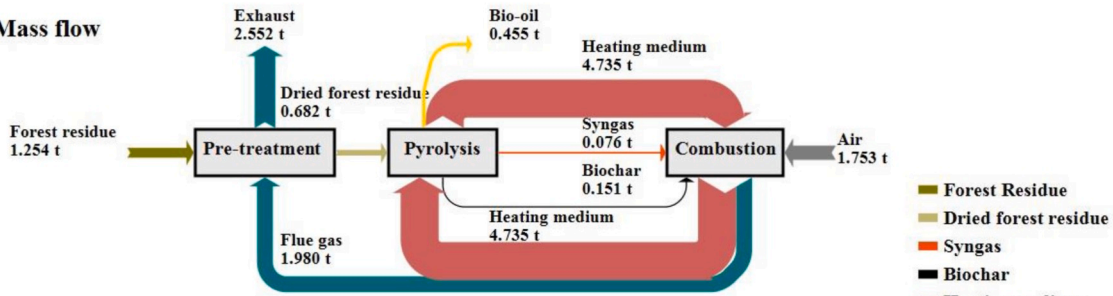


Fig. 8. Simplified (a) mass and (b) energy balance for anaerobic digestion of *L. digitata*.

Pyrolysis process

(a) Mass flow



(b) Energy flow

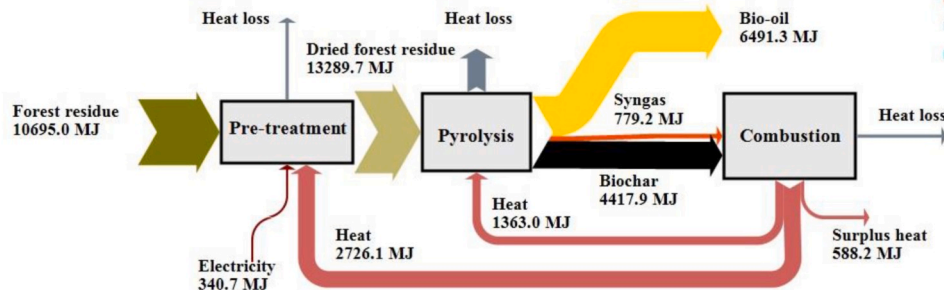


Fig. 9. Simplified (a) mass and (b) energy balance for pyrolysis of forest residue.

ture. The basic layout for a fluidizing-bed Py system processing forest residue at 500 °C for bio-oil, biochar and syngas production is designed from the available data in the work of Onarheim et al. [102]. The mass and energy balance of this Py system were analysed based on the following literature data and assumptions:

- (1) The moisture content in the forest residue is 50% and reduces to 8% after the drying process [102]. The mass yield of bio-oil, biochar, and syngas based on the dry matter of forest residue (8% moisture) are 66.7%, 22.2%, and 11.1%, respectively [102], which agrees well with other studies [99,103–105]. The LHV of the obtained bio-oil (on an organic phase basis), biochar, and

- (4) Other parameters such as the mass flow of air in the combustor, mass flow of heating medium circulating between the combustor and the pyrolysis reactor, and the mass flow of exhaust gas are adapted from the work of Onarheim et al. [102].
- (5) The energy output of the Py system includes the surplus heat produced from combustion in excess of self-consumption and the energy value of bio-oil. The process efficiency is defined as per Eq. (9).

$$\eta_{AD} = \frac{(\text{Surplus heat} \div 90\%) + \text{Energy value of bio-oil}}{\text{Energy value of forest residue} + \text{Primary energy consumption of the Py system}} \quad (\text{Eq. 9})$$

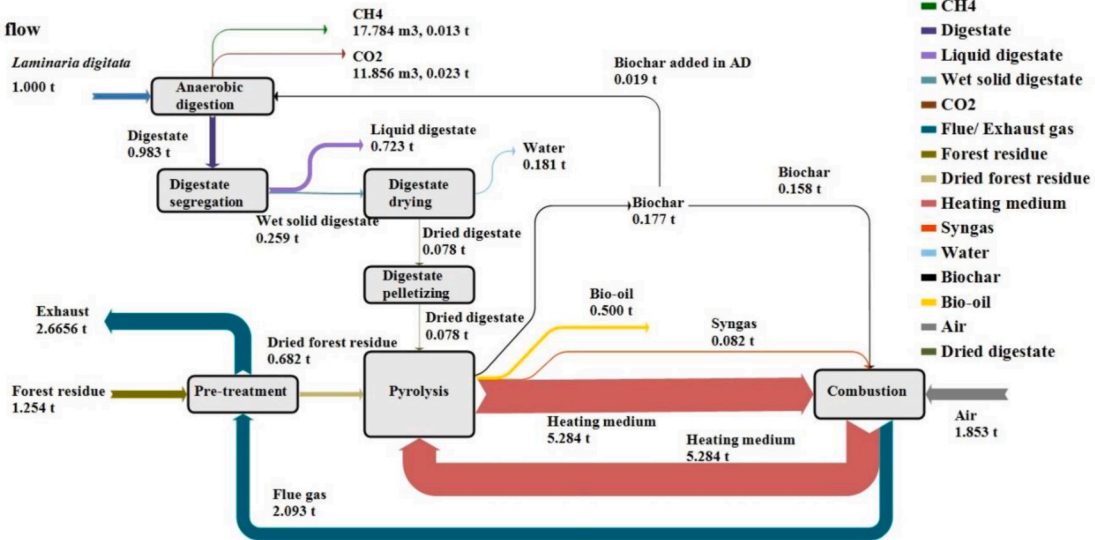
syngas are 20.4 MJ/kg, 29.2 MJ/kg, and 10.3 MJ/kg, respectively, which are calculated according to Eq. (5) based on the reported elemental composition of the products [102].

- (2) Electricity input for pre-treating forest residue (such as powering the pumps, compressor, feedstock grinding, and the belt dryer) is 0.5 MJ/kg dry matter [102]. Heat demand for drying the forest residue and for heating the pyrolysis reactor is 4.0 and 2.0 MJ/kg dry matter, respectively [102].
- (3) The produced biochar and syngas are burnt to generate heat, which is used for drying the forest residue and reheating the heating medium circulated to the pyrolysis reactor. The heat efficiency of the combustor is assumed as 90%. As the heat demand for running the system can be self-sustained by the heat produced from biochar and syngas combustion, the primary energy consumption of the Py system contains only grid electricity consumption for forest residue pre-treatment.

Table S3 in the supplementary material presents the detailed calculations. Fig. 9 shows the mass and energy balance of the Py system. The mass and energy calculations are based on processing 1.254 t forest residue with an energy value of 10659.0 MJ. This feeding parameter is determined in the design of cascading AD-Py system in section 3.4.2. The production of bio-oil, biochar, and syngas is calculated as 0.455, 0.151, and 0.076 t, respectively. The energy value of bio-oil is 6491.3 MJ. The obtained syngas and biochar are burnt to produce 4677.4 MJ of heat. In excess of the heat consumption for drying forest residue (2726.1 MJ) and heating the pyrolysis reactor (1363.0 MJ), the combustion of syngas and biochar generates significant surplus heat of 588.2 MJ which could be sold to the public via a district heating grid. The energy output of the Py system is 7133.9 MJ including the energy value of bio-oil and surplus heat. The electricity consumed for forest residue pre-treatment is 340.7 MJ, leading to a total primary energy consumption of 783.8 MJ. Therefore, the net energy gain in the Py system is 6361.2 MJ, resulting in a process efficiency of 62.4%. This result is consistent with the research

Integrated AD-Py process

(a) Mass flow



Integrated AD-Py process

(b) Energy flow

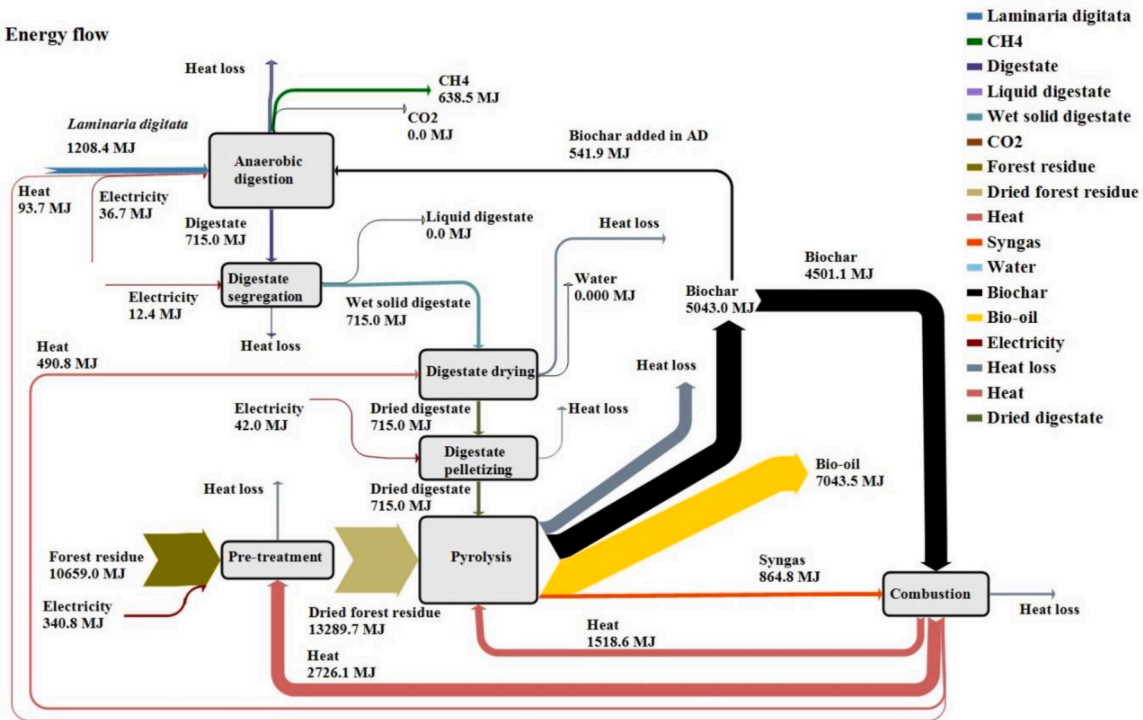


Fig. 10. Simplified (a) mass and (b) energy balance for the cascading circular anaerobic digestion and pyrolysis system.

of Onarheim et al., in which a process efficiency of 55.8% was obtained without consideration of surplus heat output [102]. Salman et al. reported a much higher process efficiency of 75% for stand-alone pyrolysis as the electricity and heat consumption were not converted into primary energy consumption in the calculation [99].

3.4.2. Mass and energy balance of integrated AD-Py system

As mentioned previously, surplus heat is produced in an individual Py system. Based on the individual AD and Py system, an integrated AD-Py system is proposed, in which the surplus heat is used in the AD system for heating the digester and drying the solid digestate. The dried digestate is pyrolyzed together with the forest residue to produce more bio-oil, biochar, and syngas. The pyrolysis of solid digestate can

contribute to not only the generation of value-added biofuels but also the reduction in the cost and greenhouse gas emissions associated with digestate management. Biochar produced in the Py system is added into the anaerobic digester to enhance biomethane production. A preliminary mass and energy balance were drawn to assess the benefits of integrating AD and Py systems based on the following assumptions:

- (1) The calculations are based on treating 1.000 t wet *L. digitata* in the AD system. Biochar produced in the Py system is added into the digester at a mass ratio to the VS in *L. digitata* of 25%.
- (2) The heat requirement for drying wet solid digestate (70% moisture content) includes the heat required to increase the temperature of digestate from 25 °C to 100 °C and the heat required for

water evaporation [106]. The electricity required for digestate pelletizing is 150 kWh/t dried solid digestate [98].

- (3) To cover all the heat demand in the AD-Py system by burning syngas and surplus biochar (in excess of the biochar added into the digester), on a per tonne basis of *L. digitata* at least 1.254 t forest residue is needed to feed the Py system together with the dried solid digestate (0.078 t). The yield of bio-oil, biochar, and syngas from forest residue remains as the yield in the individual Py process. The yield of bio-oil, biochar, and syngas from dried digestate is 58.4%, 32.8%, and 8.8% on a dry matter basis, respectively [98].
- (4) The LHV of the digestate derived bio-oil and syngas is 22.1 MJ/kg and 12.5 MJ/kg, respectively [98]. The LHV of digestate derived biochar is not specified in the same paper [98] but has been reported in a range of 21.8–27.1 MJ/kg [107–114]. These values are lower compared to that of the forest residue derived biochar due to the higher ash content in the digestate. As the characteristics of biochar produced from seaweed digestate are not available in the literature, the LHV of digestate derived biochar is modelled as 24.5 MJ/kg according to Ref. [113,114], in which the digestates showed elemental distributions similar to the *L. digitata* digestate in this study.

Table S4 in the supplementary material presents the detailed calculations of the overall integrated system. Fig. 10 shows the mass and energy balance of the integrated AD-Py system. Due to the addition of biochar, the biomethane and carbon dioxide yields from 1.000 t *L. digitata* are improved to 17.784 and 11.856 m³, respectively. In the segregation process, 0.259 t wet solid digestate and 0.723 t liquid digestate are obtained. The yield of bio-oil, biochar, and syngas is 0.500, 0.177, and 0.082 t, respectively. The energy value of bio-oil is 7043.5 MJ. The syngas and surplus biochar are burnt to produce 4829.3 MJ of heat, which can fully cover the heat demand in the integrated AD-Py system for drying the digestate and forest residue and heating the digester and pyrolysis reactor. The energy output of the AD-Py system is 7682.1 MJ including the energy value of output biomethane, bio-oil, and surplus heat from combustion. The total electricity consumption for biogas production, digestate segregation, digestate pelletizing, and forest residue pre-treatment is 431.8 MJ, leading to a total primary energy consumption of 993.2 MJ. Therefore, the net energy gain in the AD-Py system is 6688.8 MJ. The process efficiency is 59.7%, which is lower than that of the individual Py system (62.4%) but much higher than the efficiency of the individual AD system (38.1%).

The integrated AD-Py system leads to an increase of 17% in biomethane yield and an increase of 10% in bio-oil production compared to the individual AD and Py systems. The net energy gain is slightly improved by 0.1%, despite the additional energy requirement for processing digestate. Wet solid digestate (accounting for 26% of the digestate mass) from AD is valorised in the Py system, which could significantly reduce the arable land requirement for digestate spread, the cost for digestate transportation/storage, and the greenhouse gas emissions associated with land application. Monlau et al. reported that the syngas and bio-oil produced in pyrolysis of digestate could increase the electricity production of the AD plant by 42%, even though the biomethane production did not change [98]. Salman et al. [100] demonstrated an approximate 7% increase in the efficiency of a combined AD-Py process by assuming a 5% increase in methane content as a result of biochar addition into the digester. With consideration of both the pyrolysis of digestate and the effect of biochar addition on AD, the enhancement in biomethane and bio-oil production is more encouraging in the cascading circular AD-Py system proposed in this study. It should be noted that these cited studies did not take into account the primary energy factors for electricity and heat, which means that the energy calculations were not conducted on a unified primary energy baseline. In this study, the energy consumption was converted into primary energy consumption with factors of 2.3 and 1.1 for electricity and heat,

respectively, which in essence led to higher values of total primary energy consumption. If renewable electricity such as from wind, wave, and solar could be used in this integrated AD-Py system, the process efficiency would be significantly improved as the primary energy factor for renewable electricity is 1.0.

3.4.3. Future research on expansion of integrated technologies

This study demonstrated the benefits of the integration of AD and pyrolysis. However, it may have some constraints or sub-optimal operation, such as unutilised CO₂ from the AD system and uncertainty in economic, environmental, and social costs. From the technical perspective, the production of biochar with tailored properties for DIET enhancement in AD, alternative utilisation of biochar as a soil amendment for carbon sequestration, and the development of further technology integration (including biomethanation via the biological Sabatier reaction or photosynthetic micro-algae biogas upgrading [115]), offer potential opportunities for further enhanced energy production efficiency and enabling a negative emission technology system. From the policy perspective, comprehensive life cycle analysis and techno-economic assessment of the integrated system are necessary to demonstrate the environmental/economic sustainability and identify the bottlenecks in commercialisation. From the industry perspective, a multi-objective optimisation of the operational strategy including for resource allocation and logistics required to maximize profit and carbon sustainability of the entire supply chain from the resource to the market is necessary [116,117].

4. Conclusions

This study demonstrated that biochar could significantly enhance biomethane yield in AD of seaweed. In digestion of *L. digitata*, biochar addition at an optimal ratio of 1/4 enhanced biomethane yield by 17% and peak production rate by 29%, which are comparable to the effects of graphene. Similarly, the recommended biochar addition in digestion of *S. latissima* led to a 16% increase in biomethane yield and a 30% increase in peak production rate. Based on the experimental results, a cascading circular AD-Py system was proposed by integrating the AD system processing *L. digitata* and the Py system processing forest residue. A preliminary mass and energy balance analysis indicated that to self-sustain all the heat demand in the AD-Py system by burning syngas and surplus biochar (in excess of the biochar added into the digester), pyrolysis of at least 1.254 t forest residue together with 0.078 t dried solid digestate is needed based on 1.000 t *L. digitata* processed in AD. The process integration increased biomethane yield by 17% and bio-oil yield by 10%. Meanwhile, a reduction of 26% in the digestate mass flow could be achieved, which may enable significant reductions in arable land requirement, transport cost, and greenhouse gas emissions associated with digestate application.

CRedit authorship contribution statement

Chen Deng: Conceptualization, Methodology, Investigation, Writing - original draft. **Richen Lin:** Conceptualization, Methodology, Validation, Writing - review & editing. **Xihui Kang:** Investigation, Writing - review & editing. **Benteng Wu:** Investigation, Writing - review & editing. **Richard O'Shea:** Validation, Writing - review & editing. **Jerry D. Murphy:** Conceptualization, Validation, Writing - review & editing, Supervision, Funding acquisition.

Acknowledgements

This study was funded by Science Foundation Ireland (SFI) through the Centre for Energy, Climate, Marine (MaREI) under Grant No. 12/RC/2302_P2 and 16/SP/3829, the European Regional Development Fund under the Interreg NWE Project BioWILL (No. NWE 964), the European Union's Horizon 2020 research and innovation program under the Marie

Skłodowska-Curie grant (No. 797259) and the Environmental Protection Agency – Ireland (2018-RE-MS-13). Industrial co-funding from Gas Networks Ireland through the Gas Innovation Group is also gratefully acknowledged.

Appendix A. Supplementary data

Supplementary data to this article can be found online at <https://doi.org/10.1016/j.rser.2020.109895>.

References

- [1] CO₂ emissions from fuel combustion. International Energy Agency; 2019. <https://www.iea.org/subscribe-to-data-services/co2-emissions-statistics>.
- [2] Directive (EU). 2018/2001 of the European Parliament and of the Council of 11 December 2018 on the promotion of the use of energy from renewable sources. 2018.
- [3] Sudhakar K, Mamat R, Samykano M, Azmi WH, Ishak FWF, Yusaf T. An overview of marine macroalgae as bioresource. *Renew Sustain Energy Rev* 2018;91: 165–79.
- [4] Tabassum MR, Xia A, Murphy JD. Potential of seaweed as a feedstock for renewable gaseous fuel production in Ireland. *Renew Sustain Energy Rev* 2017; 68:136–46.
- [5] Montingelli ME, Tedesco S, Olabi AG. Biogas production from algal biomass: a review. *Renew Sustain Energy Rev* 2015;43:961–72.
- [6] Allen E, Wall DM, Herrmann C, Xia A, Murphy JD. What is the gross energy yield of third generation gaseous biofuel sourced from seaweed? *Energy* 2015;81: 352–60.
- [7] Thompson TM, Young BR, Baroutian S. Advances in the pretreatment of brown macroalgae for biogas production. *Fuel Process Technol* 2019;195.
- [8] Schiener P, Black KD, Stanley MS, Green DH. The seasonal variation in the chemical composition of the kelp species *Laminaria digitata*, *Laminaria hyperborea*, *Saccharina latissima* and *Alaria esculenta*. *J Appl Phycol* 2014;27: 363–73.
- [9] Ometto F, Steinhovden KB, Kuci H, Lunnbäck J, Berg A, Karlsson A, et al. Seasonal variation of elements composition and biomethane in brown macroalgae. *Biomass Bioenergy* 2018;109:31–8.
- [10] McKennedy J, Sherlock O. Anaerobic digestion of marine macroalgae: a review. *Renew Sustain Energy Rev* 2015;52:1781–90.
- [11] Ganesh Saratale R, Kumar G, Banu R, Xia A, Periyasamy S, Dattatraya Saratale G. A critical review on anaerobic digestion of microalgae and macroalgae and co-digestion of biomass for enhanced methane generation. *Bioresour Technol* 2018; 262:319–32.
- [12] Zhong W, Chi L, Luo Y, Zhang Z, Zhang Z, Wu WM. Enhanced methane production from Taihu Lake blue algae by anaerobic co-digestion with corn straw in continuous feed digesters. *Bioresour Technol* 2013;134:264–70.
- [13] Allen E, Wall DM, Herrmann C, Murphy JD. Investigation of the optimal percentage of green seaweed that may be co-digested with dairy slurry to produce gaseous biofuel. *Bioresour Technol* 2014;170:436–44.
- [14] Tabassum MR, Xia A, Murphy JD. The effect of seasonal variation on biomethane production from seaweed and on application as a gaseous transport biofuel. *Bioresour Technol* 2016;209:213–9.
- [15] Ometto F, Berg A, Björn A, Safaric L, Svensson BH, Karlsson A, et al. Inclusion of *Saccharina latissima* in conventional anaerobic digestion systems. *Environ Technol* 2018;39:628–39.
- [16] Tabassum MR, Wall DM, Murphy JD. Biogas production generated through continuous digestion of natural and cultivated seaweeds with dairy slurry. *Bioresour Technol* 2016;219:228–38.
- [17] Lin R, Deng C, Ding L, Bose A, Murphy JD. Improving gaseous biofuel production from seaweed *Saccharina latissima*: the effect of hydrothermal pretreatment on energy efficiency. *Energy Convers Manag* 2019;196:1385–94.
- [18] Thompson TM, Young BR, Baroutian S. Advances in the pretreatment of brown macroalgae for biogas production. *Fuel Process Technol* 2019;195:106151.
- [19] Ding L, Cheng J, Lin R, Deng C, Zhou J, Murphy JD. Improving biohydrogen and biomethane co-production via two-stage dark fermentation and anaerobic digestion of the pretreated seaweed *Laminaria digitata*. *J Clean Prod* 2020;251: 119666.
- [20] Ganesh Saratale R, Kumar G, Banu R, Xia A, Periyasamy S, Dattatraya Saratale G. A critical review on anaerobic digestion of microalgae and macroalgae and co-digestion of biomass for enhanced methane generation. *Bioresour Technol* 2018; 262:319–32.
- [21] Romagnoli F, Dorella M, Gruduls A, Collotta M, Tomasoni G. Anaerobic co-digestion of Baltic seaweeds with wheat straw and straw pellets: synergetic effects on biomethane yield and kinetic biodegradability constant. *Energy Procedia* 2019;158:854–60.
- [22] Milledge J, Nielsen B, Maneein S, Harvey P. A brief review of anaerobic digestion of algae for bioenergy. *Energies* 2019;12.
- [23] Obata O, Ditchfield A, Hattton A, Akunna J. Investigating the impact of inoculum source on anaerobic digestion of various species of marine macroalgae. *Algal Res* 2020;46:101803.
- [24] Adams JM, Toop TA, Donnison IS, Gallagher JA. Seasonal variation in *Laminaria digitata* and its impact on biochemical conversion routes to biofuels. *Bioresour Technol* 2011;102:9976–84.
- [25] Vanegas C, Bartlett J. Anaerobic digestion of *Laminaria digitata*: the effect of temperature on biogas production and composition. *Waste Biomass Valorization* 2012;4:509–15.
- [26] Mesnildrey L, Jacob C, Frangouides K, Reunavot M, Lesueur M. Seaweed industry in France. NETALGAE project Interreg IVb WP1 and 2 report. 2012. 2012. Available from: <http://halieutique.agrocampus-ouest.fr/pdf/3744.pdf>.
- [27] Tabassum MR, Xia A, Murphy JD. Comparison of pre-treatments to reduce salinity and enhance biomethane yields of *Laminaria digitata* harvested in different seasons. *Energy* 2017;140:546–51.
- [28] D'Este M, Alvarado-Morales M, Ciofalo A, Angelidaki I. Macroalgae *Laminaria digitata* and *Saccharina latissima* as potential biomasses for biogas and total phenolics production: focusing on seasonal and spatial variations of the algae. *Energy Fuels* 2017;31:7166–75.
- [29] Vanegas CH, Bartlett J. Green energy from marine algae: biogas production and composition from the anaerobic digestion of Irish seaweed species. *Environ Technol* 2013;34:2277–83.
- [30] Jard DJ G, Carrère H, Delgenes JP, Torrijos M, Steyer JP, Dumas C. Anaerobic digestion of macroalgae: *palmaria palmata* and *Saccharina latissima*. 13 th world congress on anaerobic digestion: recovering (bio) resources for the world. 2013. p. 25–8.
- [31] Jard G, Jackowski D, Carrère H, Delgenes JP, Torrijos M, Steyer JP, et al. Batch and semi-continuous anaerobic digestion of *Palmaria palmata*: comparison with *Saccharina latissima* and inhibition studies. *Chem Eng J* 2012;209:513–9.
- [32] Vivekanand V, Eijsink VGH, Horn SJ. Biogas production from the brown seaweed *Saccharina latissima*: thermal pretreatment and codigestion with wheat straw. *J Appl Phycol* 2011;24:1295–301.
- [33] Lamb JJ, Hjelme DR, Lien KM. Carbohydrate yield and biomethane potential from enzymatically hydrolysed *Saccharina latissima* and its industrial potential. *Adv Microbiol* 2019;9:359–71.
- [34] Lin R, Deng C, Cheng J, Xia A, Lens PNL, Jackson SA, et al. Graphene facilitates biomethane production from protein-derived Glycine in anaerobic digestion. *iScience* 2018;10:158–70.
- [35] Tian T, Qiao S, Li X, Zhang M, Zhou J. Nano-graphene induced positive effects on methanogenesis in anaerobic digestion. *Bioresour Technol* 2017;224:41–7.
- [36] Lin R, Cheng J, Zhang J, Zhou J, Cen K, Murphy JD. Boosting biomethane yield and production rate with graphene: the potential of direct interspecies electron transfer in anaerobic digestion. *Bioresour Technol* 2017;239:345–52.
- [37] Lin R, Cheng J, Ding L, Murphy JD. Improved efficiency of anaerobic digestion through direct interspecies electron transfer at mesophilic and thermophilic temperature ranges. *Chem Eng J* 2018;350:681–91.
- [38] Graphene nanosheets. Available from: <https://www.sigmaaldrich.com/catalog/product/aldrich/900439?lang=en®ion=IE>.
- [39] S J, T T. State of the biochar industry 2014: a survey of commercial activity in the biochar field. International Biochar Initiative; 2015.
- [40] Campbell RM, Anderson NM, Daugaard DE, Naughton HT. Financial viability of biofuel and biochar production from forest biomass in the face of market price volatility and uncertainty. *Appl Energy* 2018;230:330–43.
- [41] Sun T, Levin BD, Guzman JJ, Enders A, Muller DA, Angenent LT, et al. Rapid electron transfer by the carbon matrix in natural pyrogenic carbon. *Nat Commun* 2017;8:14873.
- [42] Liu Y, Dai G, Zhu L, Wang S. Green conversion of microalgae into high-performance sponge-like nitrogen-enriched carbon. *ChemElectroChem* 2019;6: 602.
- [43] Masebinu SO, Akinlabi ET, Muzenda E, Aboiyade AO. A review of biochar properties and their roles in mitigating challenges with anaerobic digestion. *Renew Sustain Energy Rev* 2019;103:291–307.
- [44] Cooney MJ, Lewis K, Harris K, Zhang Q, Yan T. Start up performance of biochar packed bed anaerobic digesters. *J Water Process Eng* 2016;9:e7–13.
- [45] Wang D, Ai J, Shen F, Yang G, Zhang Y, Deng S, et al. Improving anaerobic digestion of easy-acidification substrates by promoting buffering capacity using biochar derived from vermicompost. *Bioresour Technol* 2017;227:286–96.
- [46] Ahmed W, Sarkar B. Impact of carbon emissions in a sustainable supply chain management for a second generation biofuel. *J Clean Prod* 2018;186:807–20.
- [47] Li F, Srivatsa SC, Bhattacharya S. A review on catalytic pyrolysis of microalgae to high-quality bio-oil with low oxygenous and nitrogenous compounds. *Renew Sustain Energy Rev* 2019;108:481–97.
- [48] Council EASA. Negative emission technologies: what role in meeting Paris Agreement targets? EASAC policy report 35. Available on, <https://easac.eu/publications/details/easac-net/2018>.
- [49] Smith P. Soil carbon sequestration and biochar as negative emission technologies. *Global Change Biol* 2016;22:1315–24.
- [50] Feng Q, Lin Y. Integrated processes of anaerobic digestion and pyrolysis for higher bioenergy recovery from lignocellulosic biomass: a brief review. *Renew Sustain Energy Rev* 2017;77:1272–87.
- [51] Tabassum MR, Xia A, Murphy JD. Seasonal variation of chemical composition and biomethane production from the brown seaweed *Ascophyllum nodosum*. *Bioresour Technol* 2016;216:219–26.
- [52] Eaton AD, Clesceri LS, Greenberg AE, Franson MAH. Standard methods for the examination of water and wastewater. *Am J Public Health Nation's Health* 1995; 56:387–8.
- [53] Deng C, Lin R, Cheng J, Murphy JD. Can acid pre-treatment enhance biohydrogen and biomethane production from grass silage in single-stage and two-stage fermentation processes? *Energy Convers Manag* 2019;195:738–47.

- [54] Nizami AS, Korres NE, Murphy JD. Review of the integrated process for the production of grass biomethane. *Environ Sci Technol* 2009;43:8496–508.
- [55] Eggleston HSBL, Miwa K, Ngara T, Tanabe K. IPCC guidelines for national greenhouse gas inventories. Japan: IGES; 2006.
- [56] Madigan MT, Martinko MM, Bender KS, Buckley DH, Stahl DA. *Brock biology of microorganisms: international edition, vol. 10/E. Biology of microorganisms* 2008.
- [57] Siburian R, Sihatang H, Lumban Raja S, Supeno M, Simanjuntak C. New route to synthesize of graphene nano sheets. *Orient J Chem* 2018;34:182–7.
- [58] Chen JJ, Li WW, Li XL, Yu HQ. Improving biogas separation and methane storage with multilayer graphene nanostructure via layer spacing optimization and lithium doping: a molecular simulation investigation. *Environ Sci Technol* 2012;46:10341–8.
- [59] Zhu ZW, Zheng QR. Methane adsorption on the graphene sheets, activated carbon and carbon black. *Appl Therm Eng* 2016;108:605–13.
- [60] Palmieri V, Carmela Lauriola M, Ciasca G, Conti C, De Spirito M, Papi M. The graphene oxide contradictory effects against human pathogens. *Nanotechnology* 2017;28:152001.
- [61] Zhang J, Wang Z, Wang Y, Zhong H, Sui Q, Zhang C, et al. Effects of graphene oxide on the performance, microbial community dynamics and antibiotic resistance genes reduction during anaerobic digestion of swine manure. *Bioresour Technol* 2017;245:850–9.
- [62] Dong B, Xia Z, Sun J, Dai X, Chen X, Ni BJ. The inhibitory impacts of nano-graphene oxide on methane production from waste activated sludge in anaerobic digestion. *Sci Total Environ* 2019;646:1376–84.
- [63] Li D, Song L, Fang H, Li P, Teng Y, Li YY, et al. Accelerated bio-methane production rate in thermophilic digestion of cardboard with appropriate biochar: dose-response kinetic assays, hybrid synergistic mechanism, and microbial networks analysis. *Bioresour Technol* 2019;290:121782.
- [64] Zhang M, Li J, Wang Y. Impact of biochar-supported zerovalent iron nanocomposite on the anaerobic digestion of sewage sludge. *Environ Sci Pollut Res* 2019;26:10292–305.
- [65] Wang G, Li Q, Gao X, Wang XC. Synergetic promotion of syntrophic methane production from anaerobic digestion of complex organic wastes by biochar: performance and associated mechanisms. *Bioresour Technol* 2018;250:812–20.
- [66] Xing W, You-cai Z. A bench scale study of fermentative hydrogen and methane production from food waste in integrated two-stage process. *Int J Hydrogen Energy* 2009;34:245–54.
- [67] Amani T, Nosrati M, Mousavi SM, Kermanshahi RK. Study of syntrophic anaerobic digestion of volatile fatty acids using enriched cultures at mesophilic conditions. *Int J Environ Sci Technol* 2011;8:83–96.
- [68] Wang G, Li Q, Gao X, Wang XC. Sawdust-derived biochar much mitigates VFAs accumulation and improves microbial activities to enhance methane production in thermophilic anaerobic digestion. *ACS Sustainable Chem Eng* 2018;7:2141–50.
- [69] Sunyoto NMS, Sugiarto Y, Zhu M, Zhang D. Transient performance during start-up of a two-phase anaerobic digestion process demonstration unit treating carbohydrate-rich waste with biochar addition. *Int J Hydrogen Energy* 2019;44:14341–50.
- [70] Sunyoto NMS, Zhu M, Zhang Z, Zhang D. Effect of biochar addition on hydrogen and methane production in two-phase anaerobic digestion of aqueous carbohydrates food waste. *Bioresour Technol* 2016;219:29–36.
- [71] Shen R, Jing Y, Feng J, Luo J, Yu J, Zhao L. Performance of enhanced anaerobic digestion with different pyrolysis biochars and microbial communities. *Bioresour Technol* 2020;296:122354.
- [72] Luo C, Lü F, Shao L, He P. Application of eco-compatible biochar in anaerobic digestion to relieve acid stress and promote the selective colonization of functional microbes. *Water Res* 2015;68:710–8.
- [73] Cai J, He P, Wang Y, Shao L, Lü F. Effects and optimization of the use of biochar in anaerobic digestion of food wastes. *Waste Manag Res* 2016;34:409–16.
- [74] Sharma P, Melkania U. Biochar-enhanced hydrogen production from organic fraction of municipal solid waste using co-culture of *Enterobacter aerogenes* and *E. coli*. *Int J Hydrogen Energy* 2017;42:18865–74.
- [75] Fagbohunge MO, Herbert BM, Hurst L, Li H, Usmani SQ, Semple KT. Impact of biochar on the anaerobic digestion of citrus peel waste. *Bioresour Technol* 2016;216:142–9.
- [76] Qu Y, Ma Q, Deng J, Shen W, Zhang X, He Z, et al. Responses of microbial communities to single-walled carbon nanotubes in phenol wastewater treatment systems. *Environ Sci Technol* 2015;49:4627–35.
- [77] Chen S, Rotaru AE, Shrestha PM, Malvankar NS, Liu F, Fan W, et al. Promoting interspecies electron transfer with biochar. *Sci Rep* 2014;4:5019.
- [78] Yu L, Yuan Y, Tang J, Wang Y, Zhou S. Biochar as an electron shuttle for reductive dechlorination of pentachlorophenol by *Geobacter sulfurreducens*. *Sci Rep* 2015;5:16221.
- [79] Dang Y, Sun D, Woodard T, Wang L-Y, Nevin K, Holmes D. Stimulation of the anaerobic digestion of the dry organic fraction of municipal solid waste (OFMSW) with carbon-based conductive materials. *Bioresour Technol* 2017;238:30–8.
- [80] Barua S, Dhar BR. Advances towards understanding and engineering direct interspecies electron transfer in anaerobic digestion. *Bioresour Technol* 2017;244:698–707.
- [81] Shanmugam SR, Adhikari S, Nam H, Kar Sajib S. Effect of bio-char on methane generation from glucose and aqueous phase of algae liquefaction using mixed anaerobic cultures. *Biomass Bioenergy* 2018;108:479–86.
- [82] Zhang P, Zheng S, Liu J, Wang B, Liu F, Feng Y. Surface properties of activated sludge-derived biochar determine the facilitating effects on *Geobacter* co-cultures. *Water Res* 2018;142:441–51.
- [83] Kizito S, Wu S, Kipkemoi Kirui W, Lei M, Lu Q, Bah H, et al. Evaluation of slow pyrolyzed wood and rice husks biochar for adsorption of ammonium nitrogen from piggy manure anaerobic digestate slurry. *Sci Total Environ* 2015;505:102–12.
- [84] Takaya CA, Fletcher LA, Singh S, Anyikude KU, Ross AB. Phosphate and ammonium sorption capacity of biochar and hydrochar from different wastes. *Chemosphere* 2016;145:518–27.
- [85] Mumme J, Srocke F, Heeg K, Werner M. Use of biochars in anaerobic digestion. *Bioresour Technol* 2014;164:189–97.
- [86] Lu F, Luo C, Shao L, He P. Biochar alleviates combined stress of ammonium and acids by firstly enriching *Methanosaeta* and then *Methanosarcina*. *Water Res* 2016;90:34–43.
- [87] Pan J, Ma J, Liu X, Zhai L, Ouyang X, Liu H. Effects of different types of biochar on the anaerobic digestion of chicken manure. *Bioresour Technol* 2018;275:258–65.
- [88] Shen Y, Linville JL, Ignacio-de Leon PAA, Schoene RP, Urgun-Demirtas M. Towards a sustainable paradigm of waste-to-energy process: enhanced anaerobic digestion of sludge with woody biochar. *J Clean Prod* 2016;135:1054–64.
- [89] Lu FC, Cordiner S, Manni A, Mulone V, Rocco V, Braglia R, et al. Ampelodesmos mauritanicus pyrolysis biochar in anaerobic digestion process: evaluation of the biogas yield. *Energy* 2018;161:663–9.
- [90] Su C, Zhao L, Liao L, Qin J, Lu Y, Deng Q, et al. Application of biochar in a CIC reactor to relieve ammonia nitrogen stress and promote microbial community during food waste treatment. *J Clean Prod* 2019;209:353–62.
- [91] Lü F, Liu Y, Shao L, He P. Powdered biochar doubled microbial growth in anaerobic digestion of oil. *Appl Energy* 2019;247:605–14.
- [92] Murphy JD, McKeogh E, Kiely G. Technical/economic/environmental analysis of biogas utilisation. *Appl Energy* 2004;77:407–27.
- [93] Yuan T, Cheng Y, Zhang Z, Lei Z, Shimizu K. Comparative study on hydrothermal treatment as pre- and post-treatment of anaerobic digestion of primary sludge: focus on energy balance, resources transformation and sludge dewaterability. *Appl Energy* 2019;239:171–80.
- [94] Bauer A, Mayr H, Hopfner-Sixt K, Amon T. Detailed monitoring of two biogas plants and mechanical solid-liquid separation of fermentation residues. *J Biotechnol* 2009;142:56–63.
- [95] Al Seadi T, Drosch B, Fuchs W, Rutz D, Janssen R. 12 - biogas digestate quality and utilization. In: Wellinger A, Murphy J, Baxter D, editors. *The biogas handbook*. Woodhead Publishing; 2013. p. 267–301.
- [96] Tampio E, Marttinen S, Rintala J. Liquid fertilizer products from anaerobic digestion of food waste: mass, nutrient and energy balance of four digestate liquid treatment systems. *J Clean Prod* 2016;125:22–32.
- [97] Esser A, Sensfuss F. Review of the default primary energy factor (PEF) reflecting the estimated average EU generation efficiency referred to in Annex IV of Directive 2012/27/EU and possible extension of the approach to other energy carriers. Karlsruhe, Germany: Fraunhofer-Institut für System-und Innovationsforschung (ISI); 2016.
- [98] Monlau F, Sambusiti C, Antoniou N, Barakat A, Zabaniotou A. A new concept for enhancing energy recovery from agricultural residues by coupling anaerobic digestion and pyrolysis process. *Appl Energy* 2015;148:32–8.
- [99] Salman CA, Schwede S, Thorin E, Yan J. Enhancing biomethane production by integrating pyrolysis and anaerobic digestion processes. *Appl Energy* 2017;204:1074–83.
- [100] Salman CA, Schwede S, Thorin E, Yan J. Predictive modelling and simulation of integrated pyrolysis and anaerobic digestion process. *Energy Procedia* 2017;105:850–7.
- [101] Dave A, Huang Y, Rezvani S, McIlveen-Wright D, Novaes M, Hewitt N. Techno-economic assessment of biofuel development by anaerobic digestion of European marine cold-water seaweeds. *Bioresour Technol* 2013;135:120–7.
- [102] Onarheim K, Solantausta Y, Lehto J. Process simulation development of fast pyrolysis of wood using aspen plus. *Energy Fuels* 2014;29:205–17.
- [103] Shemfe MB, Gu S, Ranganathan P. Techno-economic performance analysis of biofuel production and miniature electric power generation from biomass fast pyrolysis and bio-oil upgrading. *Fuel* 2015;143:361–72.
- [104] Peters JF, Petrakopoulou F, Dufour J. Exergetic analysis of a fast pyrolysis process for bio-oil production. *Fuel Process Technol* 2014;119:245–55.
- [105] Karvonen J, Kunttu J, Suominen T, Kangas J, Leskinen P, Judt J. Integrating fast pyrolysis reactor with combined heat and power plant improves environmental and energy efficiency in bio-oil production. *J Clean Prod* 2018;183:143–52.
- [106] Barakat A, Chuetor S, Monlau F, Solhy A, Rouau X. Eco-friendly dry chemo-mechanical pretreatments of lignocellulosic biomass: impact on energy and yield of the enzymatic hydrolysis. *Appl Energy* 2014;113:97–105.
- [107] Inyang M, Gao B, Pullammanappallil P, Ding W, Zimmerman AR. Biochar from anaerobically digested sugarcane bagasse. *Bioresour Technol* 2010;101:8868–72.
- [108] Stefaniuk M, Oleszczuk P. Characterization of biochars produced from residues from biogas production. *J Anal Appl Pyrolysis* 2015;115:157–65.
- [109] Hung CY, Tsai WT, Chen JW, Lin YQ, Chang YM. Characterization of biochar prepared from biogas digestate. *Waste Manag* 2017;66:53–60.
- [110] Ghysels S, Ronse F, Dickinson D, Prins W. Production and characterization of slow pyrolysis biochar from lignin-rich digested stillage from lignocellulosic ethanol production. *Biomass Bioenergy* 2019;122:349–60.
- [111] Monlau F, Francavilla M, Sambusiti C, Antoniou N, Solhy A, Libutti A, et al. Toward a functional integration of anaerobic digestion and pyrolysis for a sustainable resource management. Comparison between solid-digestate and its derived pyrochar as soil amendment. *Appl Energy* 2016;169:652–62.

- [112] Monlau F, Sambusiti C, Ficara E, Aboulkas A, Barakat A, Carrère H. New opportunities for agricultural digestate valorization: current situation and perspectives. *Energy Environ Sci* 2015;8:2600–21.
- [113] Sun L, Wan S, Luo W. Biochars prepared from anaerobic digestion residue, palm bark, and eucalyptus for adsorption of cationic methylene blue dye: characterization, equilibrium, and kinetic studies. *Bioresour Technol* 2013;140:406–13.
- [114] Sun L, Wan S, Luo W. Biochars prepared from anaerobic digestion residue, palm bark, and eucalyptus for adsorption of cationic methylene blue dye: characterization, equilibrium, and kinetic studies. *Bioresour Technol* 2013;140:406–13.
- [115] Bose A, Lin R, Rajendran K, O'Shea R, Xia A, Murphy JD. How to optimise photosynthetic biogas upgrading: a perspective on system design and microalgae selection. *Biotechnol Adv* 2019;37:107444.
- [116] Sarkar B, Omair M, Choi S-B. A multi-objective optimization of energy, economic, and carbon emission in a production model under sustainable supply chain management. *Appl Sci* 2018;8.
- [117] Ahmed W, Sarkar B. Management of next-generation energy using a triple bottom line approach under a supply chain framework. *Resour Conserv Recycl* 2019;150.